Development of Small Molecules as Modulators of Amyloidogenic Peptides Associated with Alzheimer's Disease and Type II Diabetes Mellitus

Milim Jang

Department of Chemistry

Graduate school of UNIST

Development of Small Molecules as Modulators of Amyloidogenic Peptides Associated with Alzheimer's Disease and Type II Diabetes Mellitus

A thesis
Submitted to the Graduate School of UNIST
in partial fulfillment of the
requirements for the degree of
Master of Science

Milim Jang

01. 16. 2015
Approved by

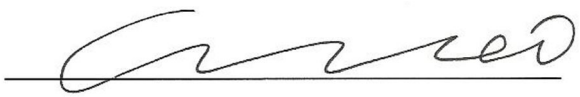

Advisor
Associate Professor Mi Hee Lim

Development of Small Molecules as Modulators of Amyloidogenic Peptides Associated with Alzheimer's Disease and Type II Diabetes Mellitus

Milim Jang

This certifies that the thesis of Milim Jang is approved.

01. 16. 2015

Signature

Advisor: Associate Professor Mi Hee Lim

Signature

Associate Professor Cheol-Min Park

Signature

Associate Professor Kyoung Taek Kim

Abstract

The progressive degenerative disorders, Alzheimer's disease (AD) and type II diabetes mellitus (T2DM), are characterized by the accumulation of misfolded peptides [*i.e.*, amyloid-β (Aβ) and human islet amyloid polypeptide (hIAPP), respectively]. In addition, multiple factors, such as metal ions and reactive oxygen species (ROS), are shown to be interconnected and involved in these peptides' aggregation and toxicity. The inter-relationship between Aβ or hIAPP, metals, ROS, and toxicity is not clear, however. In order to gain a better understanding of this interconnection, chemical tools capable of targeting metal-associated peptides and modulating their reactivities (*i.e.*, peptide aggregation, metal–peptide-induced ROS formation) have been developed. In Chapters 2 and 3, the investigations, including cytotoxicity, regulatory activity toward Aβ-/metal–Aβ-induced toxicity, and antioxidant activity, of small molecules, designed to target metal–Aβ and control their reactivities, are described. Moreover, the initial studies of metal influence on hIAPP's toxicity in living cells are discussed in Chapter 4. Overall, the overall studies in this thesis have provided insight into designing new chemical tools used for investigating multiple facets in AD and T2DM.

Contents

List of Figures

phenol; **HM2**, 4-(dimethylamino)-2-(((2-methylquinolin-8-yl)amino)methyl)phenol; **HM3**, methyl-8-((5-(dimethylamino)-2-hydroxybenzyl)amino)quinoline-2-carboxylate; **ML**, 4-(dimethyl lamino)-2-(((2-(hydroxymethyl)quinolin-8-yl)amino)methyl)phenol.

Figure 2.2. Antioxidant activity of the (a) **L2-b** and (b) **ML** derivatives determined by the TEAC assay using cell lysates. The TEAC values are relative to that of a vitamin E analogue, Trolox (6-hydroxy-2,5,7,8-tetramethylchroman-2-carboxylic acid).

Figure 2.3. Cytotoxicity studies with the **L2-b** derivatives in murine Neuro-2a neuroblastoma (N2a) cells. Cell viability upon treatment with compounds under conditions (a) without and with metal ions [(b) Cu(II) or (c) Zn(II)]. Condition: [compound] = 5–50 μM; [$CuCl_2$ or $ZnCl_2$] = 5–50 μM; 24 h; 37 °C. The values of cell viability (%), obtained by the MTT assay, were calculated compared to cells treated with DMSO only (0–1%, v/v). Error bars represent the standard error from three independent experiments.

Figure 2.4. Cytotoxicity studies with the **L2-b** derivatives in human neuroblastoma SK-N-BE(2)-M17 (M17) cells. (a) Cell viability upon incubation with compounds in the absence and presence of $CuCl_2$ or $ZnCl_2$. Cells were treated with a compound (20 μM) and/or a metal chloride salt ($CuCl_2$ or $ZnCl_2$; 20 μM) under Aβ-free conditions followed for 24 h at 37 °C. The values of cell viability (%), measured by the MTT assay after 24 h incubation, were calculated compared to cells treated only with DMSO (0–1%, v/v). Error bars represent the standard error from three independent experiments.

Figure 2.5. Cytotoxicity studies with the **ML** derivatives in murine Neuro-2a neuroblastoma (N2a) cells. Cell viability upon treatment with compounds under conditions (a) without and with (b) $CuCl_2$ or (c) $ZnCl_2$. Condition: [compound] = 5–25 μM; [$CuCl_2$ or $ZnCl_2$] = 10–20 μM; 24 h; 37 °C. The values of cell viability (%), obtained by the MTT assay, were calculated compared to cells treated only with DMSO (0–1%, v/v). The dotted lines (b and C) indicate the viability of cells incubated with $CuCl_2$ or $ZnCl_2$ (10–20 μM). Error bars represent the standard error from three independent experiments.

Figure 2.6. Cytotoxicity studies with the **ML** derivatives in human neuroblastoma SK-N-BE(2)-M17 (M17) cells. Cell viability upon treatment with compounds under conditions (a) without and with (b) $CuCl_2$ or (c) $ZnCl_2$. Cells were treated with various concentrations of compounds (5 μM, 10 μM, and 25 μM). Cells were added with compounds (10 μM) and metal ions [Cu(II) or Zn(II); 10 μM]. The values of cell viability (%), obtained by the MTT assay after 24 h incubation at 37 °C, were calculated

compared to cells treated only with DMSO (0–1%, v/v). The dotted lines (b and C) indicate the viability of cells incubated with $CuCl_2$ or $ZnCl_2$ (10 μM). Error bars represent the standard error from three independent experiments.

Figure 2.7. Effect of compounds on survival of cells incubated with metal-free Aβ and metal–Aβ. Cells were treated with $A\beta_{40}/A\beta_{42}$ [(a) 10 μM or (b) 20 μM], with/without metal ions [$CuCl_2$ or $ZnCl_2$; (a) 10 μM or (b) 20 μM], and the **L2-b** derivatives [(a) 10 μM or (b) 20 μM] for 24 h at 37 °C. (c) Effect of the **ML** derivatives on survival of cells incubated with metal-free Aβ and metal–Aβ. Cells were treated with $A\beta_{40}/A\beta_{42}$ (10 μM), with/without metal ions [$CuCl_2$ or $ZnCl_2$; 10 μM], and compounds (10 μM) for 24 h at 37 °C.

Figure 3.1. Chemical structures of glycosylated polyphenols and their derivatives. **Phlorizin**, 1-(2,4-dihydroxy-6-(((2*S*,3*R*,4*R*,6*R*)-3,4,5-trihydroxy-6-(hydroxymethyl)tetrahydro-2*H*-pyran-2-yl)oxy)phenyl)-3-(4-hydroxyphenyl)propan-1-one; **Verbascoside**, (2*R*,3*R*,4*R*,5*R*,6*R*)-6-(3,4-dihydroxy phenethoxy)-5-hydroxy-2-(hydroxymethyl)-4-(((2*S*,3*R*,4*R*,5*R*)-3,4,5-trihydroxy-6-methyltetrahydro-2*H*-pyran-2-yl)oxy)tetrahydro-2*H*-pyran-3-yl(*E*)-3-(3,4-dihydroxyphenyl)-acrylate; **Rutin**, 2-(3,4-dihydroxy phenyl)-5,7-dihydroxy-3-(((2*S*,3*R*,4*S*,5*S*,6*R*)-3,4,5-trihydroxy-6-((((2*S*,3*R*,4*R*,5*S*)-3,4,5-trihydroxyl-tetrahydro-2*H*-pyran-2-yl)oxy)methyl)tetrahydro-2*H*-pyran-2-yl)oxy)-4*H*-chromen-4-one; **F2**, (2*S*,3*R*,4*R*,6*R*)-2-(3,5-dihydroxy-2-(3-(4-hydroxyphenyl)pro-panoyl)phenoxy)-6-((propionyloxy) methyl)tetrahydro-2*H*-pyran-3,4,5-triyl tripropionate; **VPP**, (2*S*,3*R*,4*R*,5*S*)-2-(((2*R*,3*R*,4*S*,5*R*,6*R*)-2-(3,4-dihydroxyphenethoxy)-5-(((*E*)-3-(3,4-dihydroxyphenyl)acryloyl)oxy)-3-(propionyloxy)-6-((propionyloxy)methyl)tetrahydro-2*H*-pyran-4-yl)oxy)-6-methyltetrahydro-2*H*-pyran-3,4,5-triyl tripropionate; **R2**, (2*R*,3*R*,4*R*,5*S*,6*S*)-2-(((2*R*,3*R*,4*S*,5*R*,6*S*)-6-((2-(3,4-dihydroxyphenyl)-5,7-dihydroxy-4-oxo-4*H*-chromen-3-yl)oxy)-3,4,5-tris(propionyloxy)tetrahydro-2*H*-pyran-2-yl)methoxy)-6-methyltetrahydro-2*H*-pyran-3,4,5-triyl tripropionate.

Figure 3.2. Cu(II) binding studies of **Phlorizin**, **F2**, **Verbascoside**, **VPP**, **Rutin**, and **R2** observed by UV–vis. Samples were incubated for 2 h with and without Cu(II) (0.5–10 equiv) at pH 7.4 at room temperature.

Figure 3.3. Zn(II) binding of **Verbascoside** and **VPP** observed by ^{1}H NMR. Samples were incubated for 30 min with $ZnCl_2$ (0 or 1 equiv) in DMSO-d_6 at room temperature.

Figure 3.4. Antioxidant activity of **Phlorizin**, **F2**, **Verbascoside**, **VPP**, **Rutin**, and **R2** evaluated by the cell lysate-based TEAC assay. The TEAC values are relative to a vitamin E analogue, Trolox (6-

hydroxy-2,5,7,8-tetramethylchroman-2-carboxylic acid).

Figure 4.1. Cytotoxicity studies of the human islet amyloid polypeptide (IAPP) in the rat insulinoma-1 (INS-1) pancreatic β cell. Cells were treated with hIAPP [10 μM (gray bars) or 20 μM (black bars)], with/without a metal chloride salt [$CuCl_2$ or $ZnCl_2$, 70 μM (gray bars) or 140 μM (black bars)] followed by 24 h incubation at 37 °C. The values of cell viability (%), measured by the MTT assay, were calculated compared to cells treated with H_2O only. Error bars represent the standard error from three independent experiments.

Figure 4.2. Cytotoxicity studies of the Cu(II)–hIAPP in the rat insulinoma-1 (INS-1) pancreatic β cell. Cells were treated with hIAPP (20 μM) without and with $CuCl_2$ (20–100 μM) and incubated for 24 h at 37 °C. The values of cell viability (%), measured by the MTT assay, were calculated compared to cells treated with H_2O only. Error bars represent the standard error from three independent experiments.

Figure 4.3. Cytotoxicity studies with hIAPP in the rat insulinoma-1 (INS-1) pancreatic β cell. Cell viability upon incubation time [(a) 6 h or (b) 24 h] after treatment with hIAPP and metal–hIAPP preincubated for 1 h, 2 h, 3 h, and 9 h. Cells were treated with samples incubated hIAPP (10–20 μM) without and with $CuCl_2$ or $ZnCl_2$ (70–140 μM) followed by 6 h or 24 h incubation at 37 °C. The values of cell viability (%), measured by the MTT assay after 24 h incubation, were calculated compared to cells treated with HEPES only. Error bars represent the standard error from three independent experiments.

Figure 4.4. Cytotoxicity studies with the hIAPP in the rat insulinoma-1 (INS-1) pancreatic β cell. Cell viability upon treatment with metal-free hIAPP and metal–hIAPP preincubated for 3 h at 37 °C. Cells were treated with preincubated hIAPP (20 μM) with/without metal ions [(a) $CuCl_2$, 20–200 μM; (b) $ZnCl_2$, 60–200 μM] for 24 h incubation at 37 °C. The values of cell viability (%), obtained by the MTT assay, were calculated compared to cells treated with HEPES only. Error bars represent the standard error from three independent experiments.

Figure 4.5. Cytotoxicity studies with the apoptosis reagents in the rat insulinoma-1 (INS-1) pancreatic β cell. Cell viability of hIAPP treated cells upon treatment of the apoptosis inhibitors (calpeptin or trehalose) or enhancer (bafilomycin) with various concentration of a compound. Condition: [hIAPP] = 20 μM; [calpeptin] = 1.25–10 μM, [trehalose] = 100–150 mM, [bafilomycin] = 0.01–0.2 μM; 24 h; 37 °C. The values of cell viability (%), obtained by the MTT assay, were calculated compared to cells

treated with DMSO only (0–1%, v/v). Error bars represent the standard error from three independent experiments.

Figure 4.6. Cytotoxicity studies with the apoptosis reagents in the rat insulinoma-1 (INS-1) pancreatic β cell. Cells were treated with hIAPP (20 μM), with $CuCl_2$ (60 μM), and compounds (calpeptin, 2–7 μM; trehalose, 100 mM; bafilomycin, 0.01–0.05 μM) for 24 h at 37 °C. The values of cell viability (%), obtained by the MTT assay, were calculated compared to cells treated with DMSO only (0–1%, v/v). Error bars represent the standard error from three independent experiments.

Nomenclature

Aβ	Amyloid-β
ABTS	2,2‘-Azino-bis(3-ethylbenzothiaxoline-6-sulfonic acid
AD	Alzheimer’s disease
Cu	Copper
$CuCl_2$	Copper(II) chloride
DMEM	Dulbecco’s modified Eagle medium
DMSO	Dimethyl sulfoxide
FBS	Fetal bovine serum
Fe	Iron
H_2O_2	Hydrogen peroxide
HEPES	2-[4-(2-Hydroxyethyl)piperazin-1-yl]ethanesulfonic acid
K_d	Dissociation constant
M17	SK-N-BE(2)-M17
MEM	Minimal essential media
MTT	3-(4,5-Dimethylthiazol-2-yl)-2,5-diphenyltetrazolium bromide
N2a	Neuro-2a
NaCl	Sodium chloride
NEAA	Non-essential amino acids
NH_4OH	Ammonium hydroxide
NMR	Nuclear magnetic resonance
$O_2^{\bullet-}$	Superoxide anion
•OH	Hydroxyl radical
PBS	Phosphate buffered saline
ROS	Reactive oxygen species
SDS	Sodium dodecyl sulfate
UV-vis	UV-Visible spectroscopy
Vitamin E	α-Tocopherol
v/v	Volume/volume ratio
Zn	Zinc
$ZnCl_2$	Zinc(II) chloride

Chapter 1. Protein Misfolding Diseases: Alzheimer's Disease and Type II Diabetes Mellitus

1.1. Introduction

The accumulation of peptide or protein aggregates is a pathological characteristics of numerous degenerative diseases, such as Alzheimer's disease (AD), Parkinson's disease (PD), and Huntington's disease (HD), as well as metabolic diseases, including type II diabetes mellitus (T2DM).[1] These protein deposits include abnormally aggregated peptides or proteins (called amyloids) [*e.g.*, amyloid-β (Aβ) peptides and human islet amyloid polypeptides (hIAPP) for AD and T2DM, respectively].[2,3]

The aggregation of amyloidogenic peptides is depicted by the "nucleation-dependent polymerization" model which involves two kinetic phases: lag phase and elongation phase (Figure 1.1). Self assembly of the peptides generates small oligomeric and prefibrillar aggregates during the lag time. Around the end of the lag phase, these resulting, thermodynamically unstable species serve a template or nucleus for the following fibrillar growth during the elongation phase (Figure 1.1). Rapid expansion of nucleus leads to the formation of mature fibrils which are a major constituent of the peptide deposits. The kinetics of the amyloid aggregation process is sigmoidal as shown in Figure 1.1,[2,3] which is shown to be affected by various factors, including pH, temperature, agitation, and other external components (*e.g.*, metal ions, small molecules, other proteins).[4] The structure of amyloids upon aggregation is the formation and lateral stacking of β sheets along the axis of fibril growth, which can be detected by amyloid-specific dyes.[5]

Amyloid-related toxicity has been interested in studying protein misfolding diseases.[6-8] In this context, research efforts have been toward characterizing structures of amyloids, from monomers to mature fibrils, and toxic conformations.[6,8,9] Structures and kinetics of amyloids, however, depend on multiple factors, including solvents, temperature, metal ions, and small molecules, which has made amyloid-related studies challenging.[6,8,9] Such limitation on investigating chemistry of amyloids has hindered gaining a clear understanding of amyloid-triggered pathogenesis of diseases. Thus, effective therapeutics and diagnostics for amyloid-related diseases have not been developed until now. Based on the previous reports,[10] the interconnection between amyloids, metal ions, and reactive oxygen species (ROS) has been linked to toxicity. Herein, the relationship between multiple facets (*e.g.*, amyloids, metals, oxidative stress) and disease development is described.

1.2. Amyloid-β, Metals, and Oxidative Stress in Alzheimer's Disease

Alzheimer's disease (AD) is the most prevalent form of dementia and a progressive disease that is characterized by impairment of brain functions related to living and memory ability. More than 24 million people worldwide are affected with AD.[11] Over $220 billion and estimated 17.7 billion hours per a year were spent to care and support AD patients in America.[11,12] The population of the patients is predicted to increase by 40 percent by 2025.[11] Along with such serious impacts of AD on the

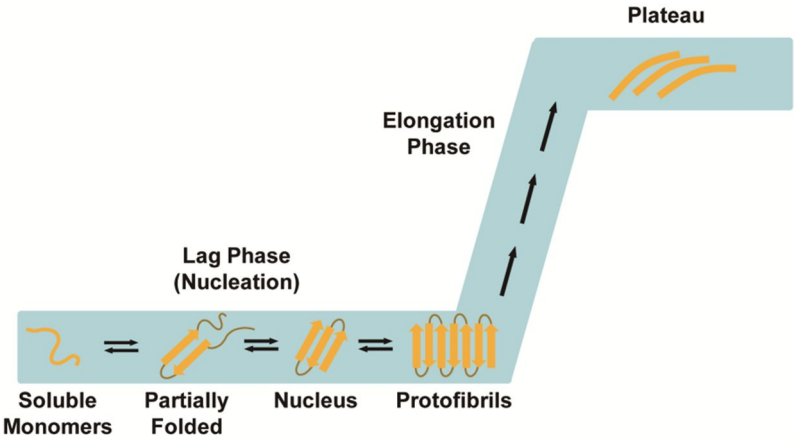

Figure 1.1. A model of the nucleation-dependent polymerization. Two phases, lag phase and elongation phase, are involved in the fibril formation. The soluble monomers are self associated to produce the initial nucleus and protofibrils during the nucleation period called lag phase. Nucleus forms are rapidly aggregated to generate fibrils in elongation phase.

economic and health care aspects in our society, the biggest concern is the lack of the cure for this disease. The currently available medications are unfortunately able only to relieve the symptoms for six months or one year. The fundamental etiology involved in AD initiation and progression has not been fully understood; thus, effective therapeutics have not been developed until now. Deposition of misfolded senile plaques and neurofibrillary tangles has a hallmark in the brain of AD. Senile plaques and fibrillary tangles are composed of aggregates of amyloid-β (Aβ) and hyperphosphorylated tau proteins, respectively.[2,3,13,14]

1.2.1. ***Amyloid-β (Aβ).*** Two major isoforms of Aβ peptides are $A\beta_{40}$ and $A\beta_{42}$ in the length of 40 and 42 amino acid residues, respectively. Aβ peptides are produced by proteolytic cleavage of the transmembrane, amyloid precursor protein (APP) (Figure 1.2).[3,23] APP can be cleaved by α-secretase, β-secretase, and γ-secretase affording to different fragmentations (Figure 1.2).[3] In the nonamyloidogenic pathway, cleavage of APP by α- and γ-secretases produces $A\beta_{17\text{-}40}$ or $A\beta_{17\text{-}42}$ (Figure 1.2). In the amyloidogenic pathway, APP is cleaved by β- and γ-secretases generating $A\beta_{1\text{-}40}$ and $A\beta_{1\text{-}42}$ (equal to $A\beta_{40}$ and $A\beta_{42}$, respectively) (Figure 1.2).[23,24]

Both $A\beta_{40}$ and $A\beta_{42}$ possess a net charge of –3 through the combination of the six negatively charged residues (D1, E3, D7, E11, E22, and D23) and the three positively charged residues (R5, K16, and K28) (Figure 1.2).[10,15] $A\beta_{42}$ has two additional hydrophobic C-terminal residues (I41 and A42) which direct the peptide more aggregation prone than $A\beta_{40}$; thus, $A\beta_{42}$ is believed more pathogenic.[15,21]

In the healthy brain, the production and clearance of Aβ is well balanced by the activity of secretases and proteases; however, this balance is not maintained in the AD-affected brain, thus

showing peptide aggregate accumulation. Currently, soluble Aβ oligomers over Aβ fibrils have been suggested to be more neurotoxic.[16,25] It is, however, still unclear whether main neurotoxic substances are fibrils or soluble oligomers.[26,27]

1.2.2. ***Metals.*** Senile plaques in the AD-affected brain are observed to contain the high level of transition metals, such as Cu, Zn, and Fe (Cu, *ca*. 0.4 mM; Zn, *ca*. 1 mM; Fe, *ca*. 0.9 mM), with comparison to that in the healthy brain tissue.[21] *In vitro* studies have shown that the increased level of metal ions is able to facilitate Aβ aggregation, suggesting that the interaction of Aβ with metal ions is involved in the process of Aβ aggregation and ROS formation leading to toxicity.[3,10,13]

Numerous studies have suggested that metal binding sites are located within 1–16 residues of Aβ.[28] Binding of Cu(II) to Aβ *in vitro* prefers a square planar geometry showing two proposed coordination modes (component I and II) that are dependent on pH.[22] Component I (Ia and Ib) is dominant at physiological pH while component II is observed at higher pH.[10] At physiological pH (component I), Cu(II) is ligated by two nitrogen (N) donor atoms from His6 and His13 or His14, a N donor atom from the N-terminal amine group, and one oxygen (O) donor atom from Ala2 (carbonyl) while the coordination of Cu(II) in component II is composed of three N donor atoms from His6, His13, and His14 and one O donor atom from Ala2 (carbonyl).[22,28,29] Binding affinity (K_d) of Cu(II) to Aβ is reported in a range of picomolar to nanomolar while K_d of Zn(II) to Aβ is approximately

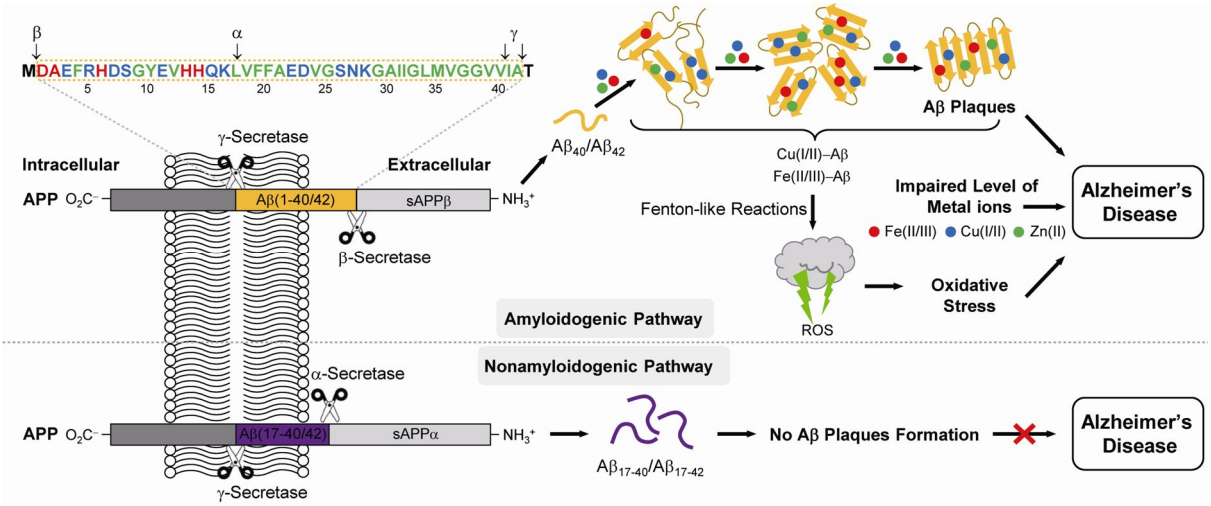

Figure 1.2. Summary of the mutual contributions of Aβ, metals, and oxidative stress to the pathogenesis of Alzheimer's disease (AD). Amyloid precursor protein (APP) is cleavaged by α-secretase, β-secretase, and γ-secretase. The nonamyloidogenic pathway is associated with activity of α-secretase and γ-secretase producing $Aβ_{17-40}$/$Aβ_{17-42}$ that do not aggregate. $Aβ_{40}$ and $Aβ_{42}$ generated through cleavage of APP by β-secretase and γ-secretase tend to aggregate (amyloidogenic pathway). $Aβ_{40}$/$Aβ_{42}$ aggregate to form oligomers and fibrills. Transition metal ions [*i.e.* Fe(II/III) (red spheres), Cu(I/II) (blue spheres), and Zn(II) (green spheres)] have been found in Aβ plaques. Redox active metal ions [*i.e.*, Cu(I/II) and Fe(II/III)] with Aβ could enhace oxidative stress *via* Fenton-like reactions forming reactive oxygen species (ROS).

micromolar.[29,30] Zn(II) is expected to coordinate with four to six ligands involving three His residues, an addition O donor atoms (from Asp1, Arg5, Glu11 or Tyr10) and an exogenous water molecule.[10,28]

1.2.3. ***Oxidative Stress Induced by Metal–Aβ.*** Redox active metal ions [*i.e.*, Cu(I/II), Fe(II/III)] are involved in Fenton-like reactions producing ROS, such as superoxide anion ($O_2^{\bullet-}$), hydrogen peroxide (H_2O_2), and hydroxyl radical (•OH) (Figure 1.3).[3] These generated ROS damage biological molecules, such as DNA, proteins, and lipids. These interactions between metals and Aβ facilitate ROS generation enhancing oxidative stress, which is considered to be a contributor to AD development.[3,10]

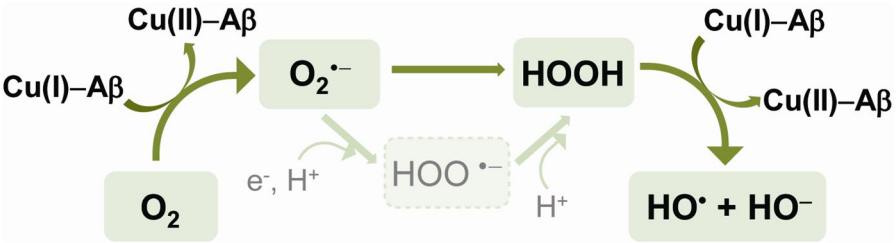

Figure 1.3. A scheme of ROS generation by copper-bound Aβ *via* Fenton-like reaction.

1.3. Human Islet Amyloid Polypeptide and Metals in Type II Diabetes Mellitus

Type II diabetes mellitus (T2DM) is a metabolic disorder that is characterized by the misregulated glucose level. Three hundred eighty two million people worldwide are estimated to suffer from this disorder by 2013.[34] Diabetes mellitus is classified into two types: type I diabetes and type II diabetes.[34] Type I diabetes mellitus (T1DM) is characterized by the disruption of pancreatic β cells caused by T-cell autoimmune attack, leading to deficiency of insulin.[2,34] On the other hand, T2DM is mainly associated with decreased insulin secretion and action as a result of insulin resistance that leads progressive dysfunction of β cells.[34,35] T2DM, formerly called noninsulin-dependent diabetes mellitus (NIDDM), is the most common form of diabetes and accounts for more than 90 % of diabetics.[2]

1.3.1. ***Human Islet Amyloid Polypeptide.*** An important causative factor of T2DM is the misfolded human islet amyloid polypeptide (hIAPP) that is a 37-residue amyloidogenic peptide, and is co-located and co-secreted with insulin in response to stimulation of pancreatic β cells.[34,36] hIAPP differs from the rat islet amyloid polypeptide (rIAPP) in only six of 37 residues, which makes different propensity of aggregation between hIAPP and rIAPP (Figure 1.4). rIAPP is known as a nonamyloidogenic peptide[37] while hIAPP has strong intrinsic propensity to aggregate to form oligomers and fibrils that are thought to be toxic to β cells despite the physiological role of hIAPP, such as glycemic regulation by reducing gastric emptying and the rate of glucose intake in blood.[4,34,36]

Several mechanisms of the fibril formation of hIAPP in T2DM have been suggested.[38] Among those, the most widely accepted mechanism is that accumulation and aggregation of hIAPP may result from its increased production and secretion by enhanced demand for insulin as a result of insulin resistance.[38] The role and mechanism of hIAPP, however, are still unclear in the pathogenesis of T2DM.[34]

Figure 1.4. The amino acid sequences of human islet amyloid polypeptide (hIAPP) and rat IAPP (rIAPP). Only six out of 37 residues in rIAPP (red) are different from the counterparts in hIAPP and peptide aggregation to form toxic species occurs for hIAPP but not rIAPP.

1.3.2. ***Metal Ions and hIAPP.*** hIAPP is observed to have a similar kinetic for its fibril formation, compared to Aβ, the nucleated growth mechanism (Figure 1.1), as well as the propensity to interact with transition metal ions [*e.g.*, Cu(I/II) and Zn(I/II)].[2] The effect of metal ions, however, have been shown to be different in aggregation rates between hIAPP and Aβ.[38,39] Zn(II) is involved in insulin synthesis, secretion, and signaling; thus Zn(II) plays an important role in glucose homeostasis as a result of insulin actions.[40,41] The role of Zn(II) on hIAPP aggregation is not fully uncovered; however, many studies have shown that Zn(II) overall has an inhibitory effect on hIAPP aggregation at physiological pH, although the effect of Zn(II) towards lag and elongation phases depends on concentration and pH.[2,4,32,39] Different from metal–Aβ interaction, Cu(II) has been shown to inhibit the formation of mature hIAPP fibrils. Similar to metal–Aβ, Cu(II)–hIAPP-mediated cytotoxicity can occur through Cu(II)-induced ROS overproduction and mitochondrial dysfunction, which could lead to apoptosis of β cells.[38]

1.4. Conclusion

AD and T2DM are two most significant forms of amyloid diseases (called amyloidosis or protein misfolding diseases). Amyloidosis, including AD and T2DM, is featured by intra- or extra-cellular deposition of misfoled peptide aggregates (Aβ and hIAPP for AD and T2DM, respectively).[2] The aggregates of these proteins share common structural traits, such as formation and lateral stacking of β sheets which are propagated along the axis of fibril growth.[5] Although numerous efforts have been made toward understanding amyloid-related pathogenesis for AD and T2DM, the identification of etiologies for both diseases has not been successful; thus, therapeutic development is still limited. Current studies present that amyloidogenic peptides, Aβ and hIAPP, can interact with metal ions showing facilitation or inhibition of their aggregation. In addition, their interactions can be linked to

production of ROS, leading to oxidative stress.[12,18,20] Therefore, the investigations on the interconnection between Aβ or hIAPP, metal ions and ROS are necessary in order to gain a better understanding of amyloid-related cytotoxicity, which will allow us to construct effective therapeutics and diagnostics for AD and T2DM.

1.5. References

(1) Ashraf, G. M.; Greig, N. H.; Khan, T. A.; Hassan, I.; Tabrez, S.; Shakil, S.; Sheikh, I. A.; Zaidi, S. K.; Akram, M.; Jabir, N. R.; Firoz, C. K.; Naeem, A.; Alhazza, I. M.; Damanhouri, G. A.; Kamal, M. A. *CNS Neurol. Disord. Drug Targets* **2014**, *13*, 1280–1293.

(2) DeToma, A. S.; Salamekh, S.; Ramamoorthy, A.; Lim, M. H. *Chem. Soc. Rev.* **2012**, *41*, 608–621.

(3) Savelieff, M. G.; Lee, S.; Liu, Y.; Lim, M. H. *ACS. Chem. Biol.* **2013**, *8*, 856–865.

(4) Salamekh, S.; Brender, J. R.; Hyung, S. J.; Nanga, R. P.; Vivekanandan, S.; Ruotolo, B. T.; Ramamoorthy, A. *J. Mol. Biol.* **2011**, *410*, 294–306.

(5) Lee, C. C.; Nayak, A.; Sethuraman, A.; Belfort, G.; McRae, G. J. *Biophys. j.* **2007**, *92*, 3448–3458.

(6) Xue, W. F.; Hellewell, A. L.; Gosal, W. S.; Homans, S. W.; Hewitt, E. W.; Radford, S. E. *J. Biol. Chem.* **2009**, *284*, 34272–34282.

(7) Selkoe, D. J. *Nat. Cell Biol.* **2004**, *6*, 1054–1061.

(8) Bemporad, F.; Chiti, F. *Chem. Biol.* **2012**, *19*, 315–327.

(9) Tenidis, K.; Waldner, M.; Bernhagen, J.; Fischle, W.; Bergmann, M.; Weber, M.; Merkle, M. L.; Voelter, W.; Brunner, H.; Kapurniotu, A. *J. Mol. Biol.* **2000**, *295*, 1055–1071.

(10) Kepp, K. P. *Chem. Rev.* **2012**, *112*, 5193–5239.

(11) 2014 Alzheimer's disease facts and figures. *Alzheimers Dement.* **2014**, *10*, 47–92.

(12) Castro, D. M. *Dement. Neuropsychol.* **2010**, *4*, 262–267.

(13) Faller, P.; Hureau, C.; Berthoumieu, O. *Inorg. Chem.* **2013**, *52*, 12193–12206.

(14) Wang, Y. J.; Zhou, H. D.; Zhou, X. F. *Drug. Discov. Today* **2006**, *11*, 931–938.

(15) Rauk, A. *Chem. Soc. Rev.* **2009**, *38*, 2698–2715.

(16) Lee, S.; Fernandez, E. J.; Good, T. A. *Protein sci.* **2007**, *16*, 723–732.

(17) Tougu, V.; Tiiman, A.; Palumaa, P. *Metallomics* **2011**, *3*, 250–261.

(18) Zhao, Y.; Zhao, B. *Oxid. Med. Cell Longev.* **2013**, *2013*, 316523–316532.

(19) Rival, T.; Page, R. M.; Chandraratna, D. S.; Sendall, T. J.; Ryder, E.; Liu, B.; Lewis, H.; Rosahl, T.; Hider, R.; Camargo, L. M.; Shearman, M. S.; Crowther, D. C.; Lomas, D. A. *Eur. J. Neurosci.* **2009**, *29*, 1335–1347.

(20) Mangialasche, F.; Solomon, A.; Winblad, B.; Mecocci, P.; Kivipelto, M. *The Lancet. Neurol.* **2010**, *9*, 702–716.

(21) Lee, S.; Zheng, X.; Krishnamoorthy, J.; Savelieff, M. G.; Park, H. M.; Brender, J. R.; Kim, J. H.; Derrick, J. S.; Kochi, A.; Lee, H. J.; Kim, C.; Ramamoorthy, A.; Bowers, M. T.; Lim, M. H. *J. Am. Chem. Soc.* **2014**, *136*, 299–310.

(22) Stellato, F.; Menestrina, G.; Serra, M. D.; Potrich, C.; Tomazzolli, R.; Meyer-Klaucke, W.; Morante, S. *Eur. Biophys. J.* **2006**, *35*, 340–351.

(23) O'Brien, R. J.; Wong, P. C. *Annu. Rev. Neurosci.* **2011**, *34*, 185–204.

(24) Zhang, Y. W.; Thompson, R.; Zhang, H.; Xu, H. *Mol. Brain* **2011**, *4*, 3–15.

(25) Bharadwaj, P. R.; Dubey, A. K.; Masters, C. L.; Martins, R. N.; Macreadie, I. G. *J. Cell. Mol. Med.* **2009**, *13*, 412–421.

(26) Benilova, I.; Karran, E.; De Strooper, B. *Nat. Neurosci.* **2012**, *15*, 349–357.

(27) Ferreira, S. T.; Vieira, M. N.; De Felice, F. G. *IUBMB life* **2007**, *59*, 332–345.

(28) Hureau, C.; Faller, P. *Biochimie* **2009**, *91*, 1212–1217.

(29) Dvinskikh, S.; Durr, U.; Yamamoto, K.; Ramamoorthy, A. *J. Am. Chem. Soc.* **2006**, *128*, 6326–6327.

(30) Choi, J. S.; Braymer, J. J.; Nanga, R. P.; Ramamoorthy, A.; Lim, M. H., *Proc. Natl. Acad. Sci. U. S. A.* **2010**, *107*, 21990–21994.

(31) Kung, H. F.; Lee, C. W.; Zhuang, Z. P.; Kung, M. P.; Hou, C.; Plossl, K. *J. Am. Chem. Soc.* **2001**, *123*, 12740–12741.

(32) Hyung, S. J.; DeToma, A. S.; Brender, J. R.; Lee, S.; Vivekanandan, S.; Kochi, A.; Choi, J. S.; Ramamoorthy, A.; Ruotolo, B. T.; Lim, M. H. *Proc. Natl. Acad. Sci. U. S. A.* **2013**, *110*, 3743–3748.

(33) Shimmyo, Y.; Kihara, T.; Akaike, A.; Niidome, T.; Sugimoto, H. *J. Neurosci. Res.* **2008**, *86*, 368–377.

(34) Marzban, L.; Park, K.; Verchere, C. B. *Exp. Gerontol.* **2003**, *38*, 347–351.

(35) Lin, Y.; Sun, Z. *J. Endocrinol.* **2010**, *204*, 1–11.

(36) Gong, H.; Zhang, X.; Cheng, B.; Sun, Y.; Li, C.; Li, T.; Zheng, L.; Huang, K. *PLoS One* **2013**, *8*, e54198–e54207.

(37) Liang, G.; Zhao, J.; Yu, X.; Zheng, J. *Biochem.* **2013**, *52*, 1089–1100.

(38) Ma, L.; Li, X.; Wang, Y.; Zheng, W.; Chen, T. *J. Inorg. Biochem.* **2014**, *140*, 143–152.

(39) Ward, B.; Walker, K.; Exley, C. *J. Inorg. Biochem.* **2008**, *102*, 371–375.

(40) Taylor, C. G. *Biometals* **2005**, *18*, 305–312.

(41) Jayawardena, R.; Ranasinghe, P.; Galappatthy, P.; Malkanthi, R.; Constantine, G.; Katulanda, P. *Diabetol. Metab. Syndr.* **2012**, *4*, 13–24.

Chapter 2. Biological Studies of Small Molecules Rationally Designed to Target and Modulate Multiple Facets of Alzheimer's Disease

2.1. Introduction

Alzheimer's disease (AD) is the most common form of dementia and the progressive brain disorder that lead to a loss of memory, thinking, and the other brain functions. More than 24 million people worldwide suffer from this disorder.[1,2] A treatment for AD, however, has not been developed yet because the etiology of the disease has been unclear. The hallmark of AD is the deposition of amyloid-β (Aβ) plaques and neurofibrillary tangles.[3-5] In the AD-affected brain, the production and clearance of Aβ peptides are mismatched so that Aβ peptides are accumulated and tend to aggregate. Among various conformations of Aβ, oligomeric forms have been suggested to be mainly responsible for toxicity in AD.[6,7] In addition, Aβ plaques contain high concentration of transition metals (*e.g.*, Cu, *ca*. 0.4 mM; Zn, *ca*. 1 mM; Fe, *ca*. 0.9 mM) in the comparison to those in healthy brain tissues (*e.g.*, Cu, *ca*. 70 μM; Zn, *ca*. 300 μM; Fe, *ca*. 300 μM).[8,9] These metal ions are observed to facilitate Aβ aggregation. In the case of redox active metal ions [*i.e.*, Cu(I/II)], metal-bound Aβ species are shown to generate reactive oxygen species (ROS) *via* Fenton-like reactions leading to oxidative stress.[10-12] Metal–Aβ species have been proposed as an interconnector of these multiple factors (*e.g.*, Aβ, metals, ROS). In that context, the design of the compounds that can target metal–Aβ species and modulate their reactivities [*i.e.*, Aβ aggregation, ROS production] is valuable to elucidate the role of metal–Aβ in AD pathogenesis. We have rationally developed compounds to target and regulate the multiple facets *via* the incorporation approach that a metal chelation moiety is integrated into an Aβ interaction framework in a single entity. For this effort, two classes of small molecules (**L2D** and **ML** derivatives, Figure 2.1) have been newly prepared and characterized. Herein, our studies of understanding a relationship between chemical structures, antioxidant activity, and cytotoxicity are presented along with their influence on cytotoxicity induced by metal-free and metal-associated Aβ.

2.2. Results and Discussion

2.2.1. Design Principle of the L2-b and ML Derivatives. The structures of **L2-b**, **ML**, and their derivatives are depicted in Figure 2.1. All ligands have structural portions for both metal chelation and Aβ interaction (Figure 2.1a, blue and green dotted line, respectively) in order to interact with metal-free Aβ and/or metal–Aβ species. In the series of **L2-b**, three major modifications were made in the backbone of **L2-b**. **L2D1**, **L2D4**, **L2D6**, **L2D10**, and **L2-nitro** are first designed to have structural variation on the dimethyl amino group of **L2-b**. This functionality is known to be critical for Aβ interaction.[13,14] Secondly, **L2D7** and **L3-b** are produced by introduction of a methyl or azo moiety on the central portion of **L2-b**. Lastly, **L2D3**, **L2D8**, and **L2D9** were constructed through the

replacement of the pyridine ring on **L2-b** with an extended aromatic ring structure, pyrrole, and mono-*N*-methylated imidazole, respectively. As shown in Figure 2.1b, **ML** is a tetradentate ligand that has strong binding affinities for Cu(II) and Zn(II) (10^{15} M^{-1} and 10^{11} M^{-1}, respectively),[9] which could be too high to chelate out metal ions from metal–Aβ species and/or metalloproteins. In order to tune metal binding, three chemical classes were prepared (Figure 2.1b): (i) 8-Aminoqiunoline derivatives (**H1**, **H2**, **H3**, and **H4**); (ii) 2-((quinolin-8-ylamino)methyl)phenol derivatives (**HM1a**, **HM2a**, **HM3a**, and **HM4a**); (iii) **ML** derivatives (**HM1**, **HM2**, **HM3**, and **ML**).

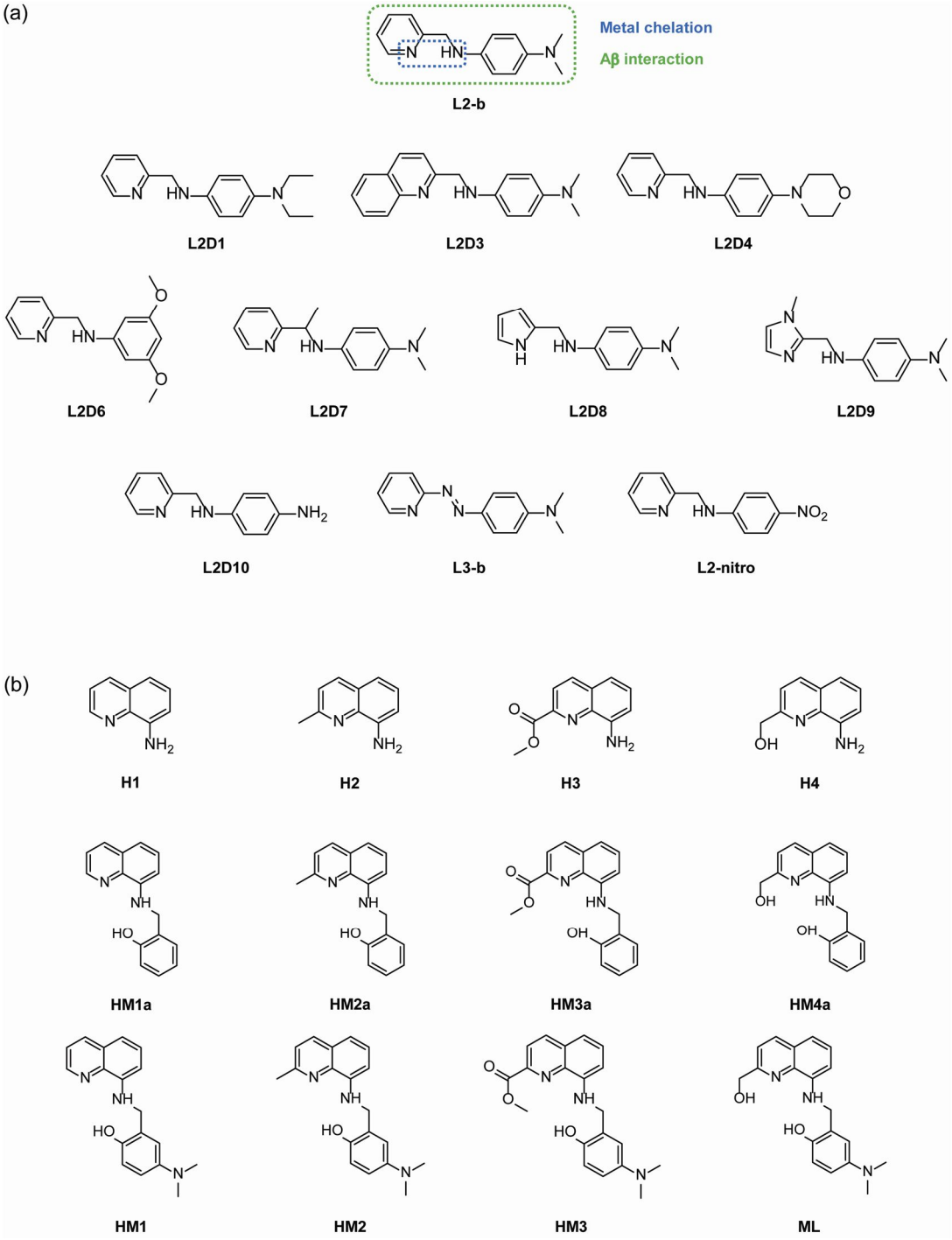

Figure 2.1. Chemical structures of **L2-b**, **ML**, and their deriatives. **L2-b**, 4-nitro-*N*-(pyridin-2-ylmethyl)aniline; **L2D1**, N^1,N^1-diethyl-N^4-(pyridin-2-ylmethyl)benzene-1,4-diamine; **L2D3**, N^1,N^1-dimethyl-N^4-(quinolin-2-ylmethyl)benzene-1,4-diamine; **L2D4**, 4-morpholino-*N*-(pyridin-2-ylmethyl) aniline; **L2D6**, 3,5-dimethoxy-*N*-(pyridin-2-ylmethyl)aniline; **L2D7**, N^1,N^1-dimethyl-N^4-(1-(pyridin-2-yl)ethyl)benzene-1,4-diamine; **L2D8**, N^1-((1H-pyrrol-2-yl)methyl)-N^4,N^4-dimethylbenzene-1,4-di amine; **L2D9**, N^1,N^1-dimethyl-N^4-((1-methyl-1H-imidazol-2-yl)methyl)benzene-1,4-diamine; **L2D10**, N^1-(pyridin-2-ylmethyl)benzene-1,4-diamine; **L3-b**, (E)-*N*,*N*-dimethyl-4-((pyridin-2-yl methylene) amino)aniline; **L2-nitro**, 4-nitro-*N*-(pyridin-2-ylmethyl)aniline; **H1**, quinolin-8-amine; **H2**, 2-methyl quinolin-8-amine; **H3**, methyl-8-aminoquinoline-2-carboxylate; **H4**, (8-aminoquinolin-2-yl)methanol; **HM1a**, 2-((quinolin-8-ylamino)methyl)phenol; **HM2a**, 2-(((2-methylquinolin-8-yl)amino)methyl) phenol; **HM3a**, methyl-8-((2-hydroxybenzyl)amino)quinoline-2-carboxylate; **HM4a**, 2-(((2-(hydroxy methyl)quinolin-8-yl)amino)methyl)phenol; **HM1**, 4-(dimethylamino)-2-((quinolin-8-ylamino)methyl) phenol; **HM2**, 4-(dimethylamino)-2-(((2-methylquinolin-8-yl)amino)methyl)phenol; **HM3**, methyl-8-((5-(dimethylamino)-2-hydroxybenzyl)amino)quinoline-2-carboxylate; **ML**, 4-(dimethyl lamino)-2-(((2-(hydroxymethyl)quinolin-8-yl)amino)methyl)phenol.

2.2.2. Antioxidant Capacity of the L2-b and ML Derivatives. In order to assess the ability of compounds to scavenge free radicals, the Trolox equivalent antioxidant capacity (TEAC) assay using cell lysates was conducted.[15,16] This assay measures the amount of ABTS cation radicals [$ABTS^{\bullet+}$; ABTS = 2,2'-azino-bis(3-ethylbenzothiazoline-6-sulfonic acid)] in the absence and presence of compounds. **L2D1**, **L2D3**, **L2D4**, **L2D6**, **L2D7**, **L2D8**, **L2D9**, **L2D10**, and **L2-b** were observed to have greater antioxidant activity than a vitamin E analogue, Trolox (6-hydroxy-2,5,7,8-tetramethylchroman-2-carboxylic acid) (Figure 2.2a). The ability of **L3-b** and **L2-nitro** to scavenge free radicals was not indicated. The azo group of **L3-b** may affect the stability of its overall structure thus preventing it from donating hydrogen or electron to radicals.[17] The nitro group of **L2-nitro** is an electron withdrawing group, which makes the overall structure difficult to quench free radicals.[17] In the case of the **ML** derivatives, the TEAC values of **HM4a**, **HM1**, **HM2**, **HM3**, and **ML** were observed to be much higher than that of Trolox by *ca*. 2.5- to 4-fold (Figure 2.2b). **H1**, **H2**, **H4**, **HM1a**, and **HM2a** indicated an antioxidant activity better than Trolox by a factor of *ca*. 1.5~2.0. **H3** showed similar ability to scavenge free radicals that of Trolox. In contrary, the antioxidant property of **HM3a** was not presented; thus dimethylamino group of **ML** derivatives may play an important role to scavenge free radicals. Overall, our results suggest that the amino group or dimethylamino group could be necessary for achieving antioxidant activity of small molecules.

2.2.3. Cytotoxicity of the L2-b and ML Derivatives. Murine Neuro-2a neuroblastoma (N2a) cells were treated with various concentrations of compounds (5–50 μM) and incubated for 24 h in a humidified atmosphere with 5% CO_2 at 37 °C. Cell survival was measured by the MTT assay [MTT = 3-(4,5-dimethylthiazol-2-yl)-2,5-diphenyltetrazolium bromide]. From the **L2-b** derivatives, among the ligands modified on the dimethylamino group of **L2-b**, **L2D1** and **L2D6** showed a similar trend in cytotoxicity to **L2-b** as a function of concentration while **L2D4** and **L2D10** were indicated to be less toxic at higher concentrations (*i.e.*, 50 μM) than **L2-b** (Figure 2.3a). Note that optical interference

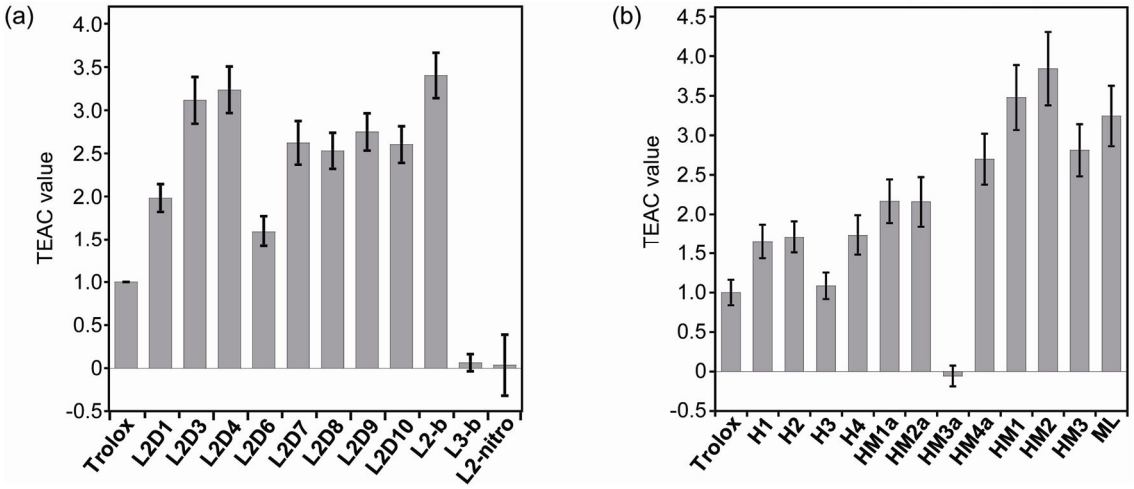

Figure 2.2. Antioxidant activity of the (a) **L2-b** and (b) **ML** derivatives determined by the TEAC assay using cell lysates. The TEAC values are relative to that of a vitamin E analogue, Trolox (6-hydroxy-2,5,7,8-tetramethylchroman-2-carboxylic acid).

with MTT at 600 nm may show increased absorbance values from the samples containing **L2D4** or **L2D10** at higher concentrations. Upon addition of cells with **L2D7** and **L3-b**, lower cell survival was observed than **L2-b** (Fig 2.3a). In the case of **L2D3** and **L2D8**, cell viability was decreased when their concentrations were increased; however, **L2D9** was indicated to be less toxic than **L2-b**, **L2D3**, and **L2D8** (Figure 2.3a). The replacement of pyridine in **L2-b** with mono-*N*-methylated imidazole is shown to influence on cell survival more than that with pyrrole (for **L2D8**) or an additional aromatic ring moiety (for **L2D3**). In the presence of metal ions, cytotoxicity of the compounds was also investigated (Figures 2.3b and 2.3c). N2a cells were treated with a metal chloride salt [$CuCl_2$ or $ZnCl_2$] and a compound in a ratio of 1:1 for 24 h. The overall cell viability with the compounds was decreased in the presence of Cu(II) (Figure 2.3b). On the other hand, incubation of cells with Zn(II) and compounds was not observed to be toxic depending on ligand concentration (Figure 2.3c).

In order to further determine a structure-toxicity relationship, cytotoxicity studies were carried out in a different cell line, human neuroblastoma SK-N-BE(2)-M17 (M17) cell line. M17 cells were first treated with or without metal ions [Cu(II) or Zn(II), 20 μM] and compounds (20 μM). Overall, small molecules, except for **L2D1**, **L2D3**, **L2D8**, and **L2-nitro**, showed slightly increased or similar cell viability (Figure 2.4), compared to that observed in N2a cells (Figure 2.3a–c). **L2D1** presented higher cell viability in the absence and presence of Zn(II) than that with Cu(II) (Figure 2.4). This tendency of cell viability is contrast to that shown in N2a cells (Figures 2.3b and 2.3c). Cells treated with **L2D3** and **L2D8** in the presence of Cu(II) showed lower cell survival unlike N2a cells at similar concentration conditions (*e.g.*, compound 20 μM for M17 cells and 25 μM for N2a cells) (Figures 2.3b and 2.4). Upon additioof **L2-nitro** to metal-free or metal-treated M17 cells, *ca*. 65–70% cell viability was observed (Figure 2.4), indicating the nitro group may cause more cytotoxicity than the dimethylamino functionality in **L2-b**.

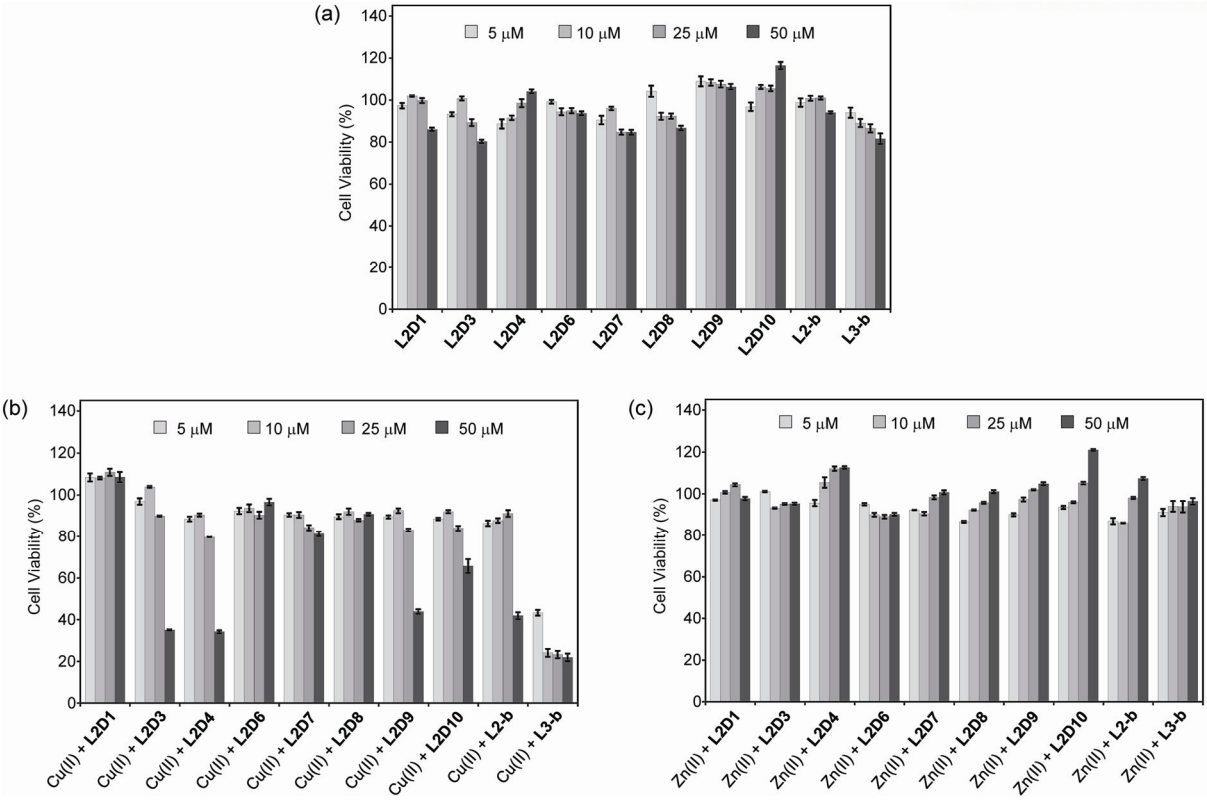

Figure 2.3. Cytotoxicity studies with the **L2-b** derivatives in murine Neuro-2a neuroblastoma (N2a) cells. Cell viability upon treatment with compounds under conditions (a) without and with metal ions [(b) Cu(II) or (c) Zn(II)]. Condition: [compound] = 5–50 μM; [$CuCl_2$ or $ZnCl_2$] = 5–50 μM; 24 h; 37 °C. The values of cell viability (%), obtained by the MTT assay, were calculated compared to cells treated with DMSO only (0–1%, v/v). Error bars represent the standard error from three independent experiments.

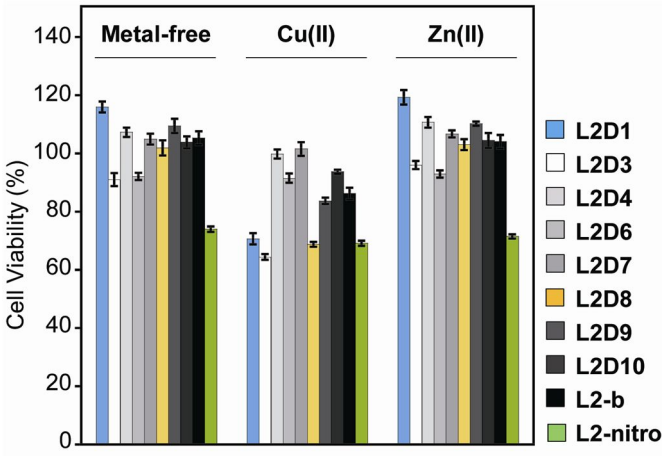

Figure 2.4. Cytotoxicity studies with the **L2-b** derivatives in human neuroblastoma SK-N-BE(2)-M17 (M17) cells. (a) Cell viability upon incubation with compounds in the absence and presence of $CuCl_2$ or $ZnCl_2$. Cells were treated with a compound (20 μM) and/or a metal chloride salt ($CuCl_2$ or $ZnCl_2$; 20 μM) under Aβ-free conditions followed for 24 h at 37 °C. The values of cell viability (%), measured by the MTT assay after 24 h incubation, were calculated compared to cells treated only with DMSO (0–1%, v/v). Error bars represent the standard error from three independent experiments.

In the case of the **ML** derivatives, cell viability of **ML** and its derivatives was also determined. The toxicity of compounds was first investigated with their multiple concentrations (5 μM, 10 μM, and 25 μM) in both N2a and M17 cell lines. Upon addition of compounds, N2a cells indicated similar cell viability (close to *ca*. 100%) (Figure 2.5a). On the contrary, the **ML** derivatives exhibited approximately 20 % decreased cell viability (Figure 2.6a). Especially, **HM2a**, **HM3a**, **HM1**, **HM2**, and **HM3** showed noticeably reduced cell survival at 25 μM (Figure 2.6a). Furthermore, upon addition of compounds, Cu(II)-treated cells were shown to be less survived with comparison to cells incubated only with compounds without metal ions (Figures 2.5b and 2.6b). Different from Cu(II), *ca*. 90–100% cell viability was observed from cells treated with Zn(II) and most of compounds (except for **HM3a** in M17 cells) (Figures 2.5c and 2.6c). Taken together, in both N2a and M17 cell lines, similar cell viability with compounds was indicated despite structural variation. In addition, compounds were shown to be relatively toxic in M17 cells in the absence and presence of metal ions (Figures 2.6b and 2.6c)

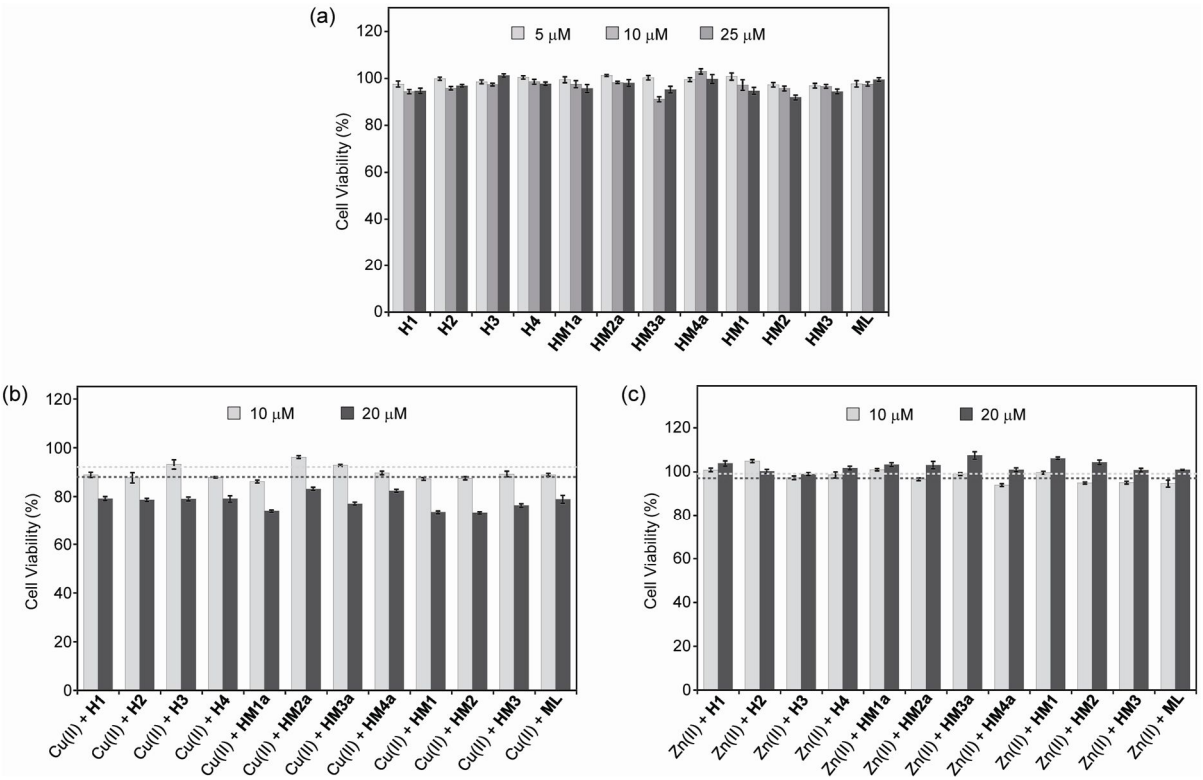

Figure 2.5. Cytotoxicity studies with the **ML** derivatives in murine Neuro-2a neuroblastoma (N2a) cells. Cell viability upon treatment with compounds under conditions (a) without and with (b) $CuCl_2$ or (c) $ZnCl_2$. Condition: [compound] = 5–25 μM; [$CuCl_2$ or $ZnCl_2$] = 10–20 μM; 24 h; 37 °C. The values of cell viability (%), obtained by the MTT assay, were calculated compared to cells treated only with DMSO (0–1%, v/v). The dotted lines (b and C) indicate the viability of cells incubated with $CuCl_2$ or $ZnCl_2$ (10–20 μM). Error bars represent the standard error from three independent experiments

2.2.4. Influence of the L2-b and ML Derivatives on Cytotoxicity Induced by Metal-free Aβ and Metal–Aβ.

The ability of compounds to regulate cytotoxicity induced by metal-free Aβ and metal–Aβ was determined in N2a cells. Note that **L3-b** was not included for this study due to its own toxicity with or without Cu(II) (Figure 2.3). From Aβ-treated N2a cells, *ca*. 90–95% cell viability with and without metal ions was observed (Figure 2.7a). Upon addition of compounds, cytotoxicity induced by $A\beta_{40}/A\beta_{42}$ and metal–$A\beta_{40}/A\beta_{42}$ was regulated by **L2D1**, **L2D3**, **L2D4**, **L2D7**, **L2D8**, **L2D9**, **L2D10**, and **L2-b** to different extents. Under metal-free conditions, most of the ligands (except for **L2D3** and **L2D8**) mitigated cytotoxicity of Aβ ($A\beta_{40}$ or $A\beta_{42}$) by 5–15% while cell viability was not recovered by **L2D3** and **L2D8** with $A\beta_{40}$ and $A\beta_{42}$ treated living cells after treatment of ligands (Figure 2.7a). The noticeable effect on attenuation in cytotoxicity was not observed by compounds for Cu(II)–Aβ (particularly, $A\beta_{42}$), although several ligands (**L2D4**, **L2D6**, **L2D7**, **L2D10**, and **L2-b**) triggered an increase in the viability of Cu(II)–$A\beta_{40}$-treated cells. In contrary, all ligands showed the ability to suppress Zn(II)–Aβ-induced cytotoxicity (Figure 2.7a). Using M17 cells, modulation of Aβ-/metal–Aβ-induced toxicity by the **L2-b** derivatives was also confirmed (Figure 2.7b).

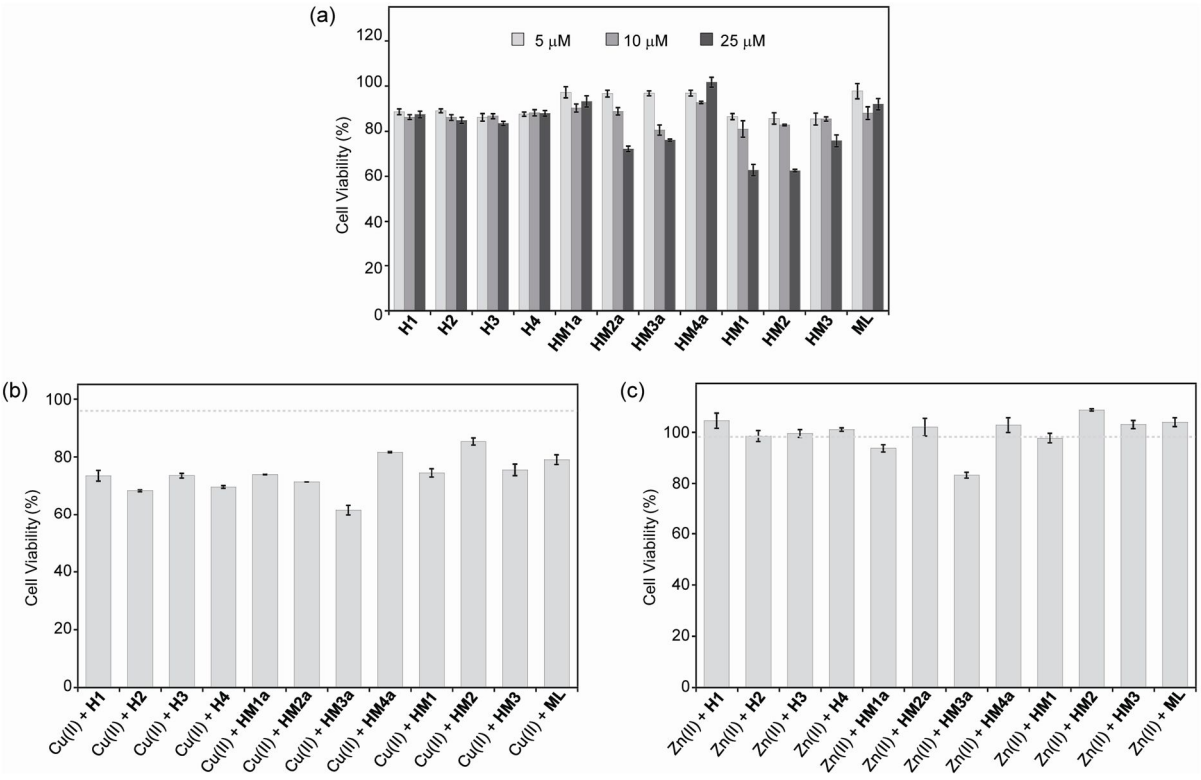

Figure 2.6. Cytotoxicity studies with the **ML** derivatives in human neuroblastoma SK-N-BE(2)-M17 (M17) cells. Cell viability upon treatment with compounds under conditions (a) without and with (b) $CuCl_2$ or (c) $ZnCl_2$. Cells were treated with various concentrations of compounds (5 μM, 10 μM, and 25 μM). Cells were added with compounds (10 μM) and metal ions [Cu(II) or Zn(II); 10 μM]. The values of cell viability (%), obtained by the MTT assay after 24 h incubation at 37 °C, were calculated

compared to cells treated only with DMSO (0–1%, v/v). The dotted lines (b and C) indicate the viability of cells incubated with $CuCl_2$ or $ZnCl_2$ (10 μM). Error bars represent the standard error from three independent experiments.

In the case of the **ML** derivatives, the effect of small molecules to regulate toxicity induced by metal-free Aβ/metal–Aβ was investigated in N2a cells. Cells were treated with Aβ (10 μM) and compounds [**HM3a**, **HM4a**, **HM1**, **HM2**, **HM3**, and **ML** (10 μM)] in the absence and presence of metal ions [Cu(II) or Zn(II), 10 μM]. All compounds, except for **HM3a**, were shown to mitigate cytotoxicity upon introduction of Aβ/metal–Aβ (Figure 2.7c). Overall, Aβ-/metal–Aβ-induced cytotoxicity was attenuated by **L2-b**, **ML** and their derivatives to different extents, which might be affected by structural variables of ligands.

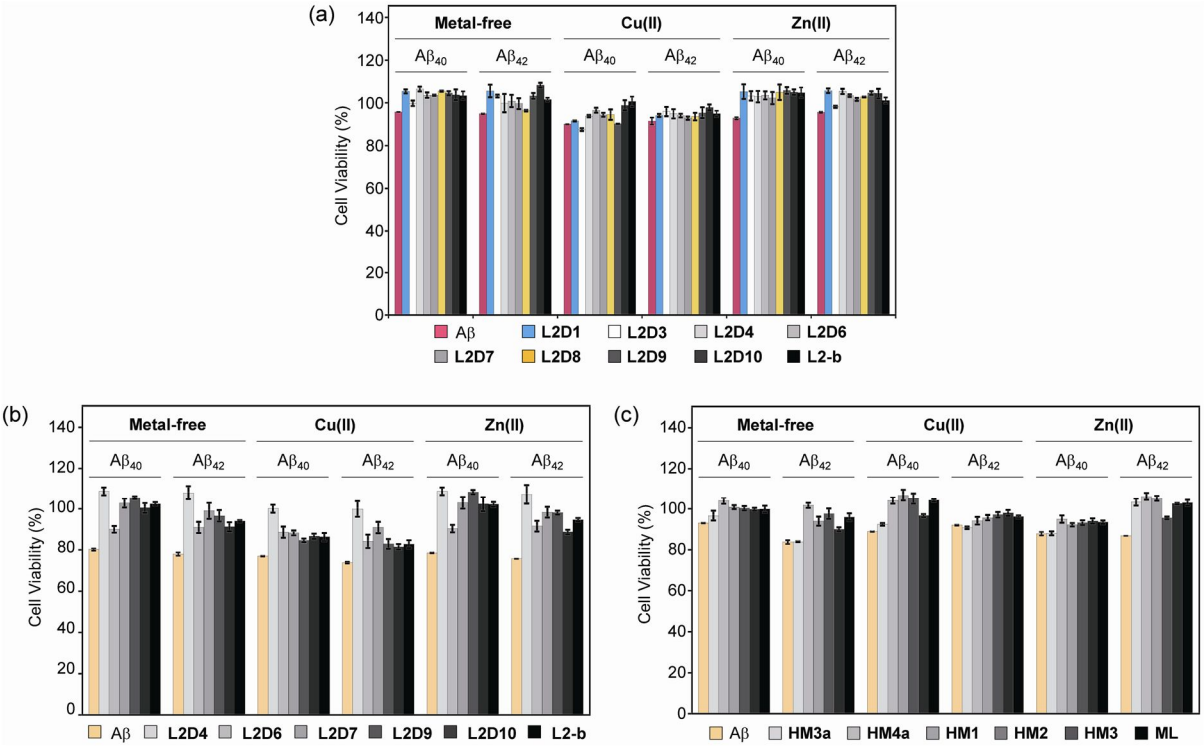

Figure 2.7. Effect of compounds on survival of cells incubated with metal-free Aβ and metal–Aβ. Cells were treated with $Aβ_{40}/Aβ_{42}$ [(a) 10 μM or (b) 20 μM], with/without metal ions [$CuCl_2$ or $ZnCl_2$; (a) 10 μM or (b) 20 μM], and the **L2-b** derivatives [(a) 10 μM or (b) 20 μM] for 24 h at 37 °C. (c) Effect of the **ML** derivatives on survival of cells incubated with metal-free Aβ and metal–Aβ. Cells were treated with $Aβ_{40}/Aβ_{42}$ (10 μM), with/without metal ions [$CuCl_2$ or $ZnCl_2$; 10 μM], and compounds (10 μM) for 24 h at 37 °C.

2.3. Conclusions

We have designed small molecules that can target and regulate multiple factors (*e.g.*, Aβ/metal–Aβ, metal ions, free radicals) that are suggested to contribute to AD development. In particular, the development of small molecules showing minimal toxicity and beneficial antioxidant

activity is challenging but valuable to be potential candidates for future biological use. In this chapter, our studies of elucidating a relationship between chemical structures (the **L2-b** and **ML** derivatives), antioxidant activity, and cytotoxicity are described. The **L2-b**/**ML** derivatives were shown to exhibit antioxidant activity and cytotoxicity although the structural modifications from the parent molecules to different extents. Our results and observations regarding a structure-antioxidant activity-cytotoxicity relationship could provide guidance in designing small molecules applicable for biological applications.

2.4. Experimental Sections

2.4.1. Aβ Preparation. Aβ peptides were dissolved in ammonium hydroxide (NH_4OH, 1% v/v, aq), aliquoted, lyophilized overnight, and stored at –80 °C. A stock solution of Aβ was prepared by dissolving the lyophilized peptide in 1% NH_4OH (10 μL) followed by dilution with ddH_2O. The concentration of Aβ peptides in the solution was determined by measuring the absorbance of the solution at 280 nm (ε = 1450 and 1490 $M^{-1}cm^{-1}$ for $A\beta_{40}$ and $A\beta_{42}$, respectively).

2.4.2. Trolox Equivalent Antioxidant Capacity (TEAC) Assay. The antioxidant activity was determined by the TEAC assay employing cell lysates following the protocol of the antioxidant assay kit purchased from Cayman Chemical Company (Ann Arbor, MI, USA) with modifications.[16,18] The N2a cells were used for this assay. This cell line purchased from the American Type Culture Collection (ATCC, Manassas, VA, USA) was maintained in media containing 50% Dulbecco's modified Eagle's medium (DMEM) and 50% OPTI-MEM (GIBCO), supplemented with 10% fetal bovine serum (FBS, Sigma), 1% non-essential amino acids (NEAA, GIBCO), 2 mM glutamine, 100 U/ml penicillin, and 100 mg/ml streptomycin (GIBCO). The cells were grown and maintained at 37 °C in a humidified atmosphere with 5% CO_2. For the antioxidant assay using cell lysates, cells were seeded in a 6 well plate and grown to approximately 80–90% confluence. Cell lysates were prepared following the previously reported method with modifications.[19] N2a cells were washed once with cold PBS (pH 7.4, GIBCO) and harvested by gently pipetting off adherent cells with cold PBS. The cell pellet was generated by centrifugation (2,000 x g for 10 min at 4 °C). This cell pellet was sonicated on ice (5 sec pulses, 5 times with 20 sec intervals between each pulse) in 2 mL of cold Assay Buffer (5 mM potassium phosphate, pH 7.4, containing 0.9% n and 0.1% glucose). The cell lysates were centrifuged at 5,000 x g for 10 min at 4 °C. The supernatant was removed and stored on ice until use. To standard and sample 96 wells, 10 μL of the supernatant of cell lysates was delivered followed by addition of compound, metmyoglobin, ABTS, and hydrogen peroxide in order. After 5 min incubation at room temperature on a shaker, absorbance values at 750 nm were recorded. The final concentrations (0.015, 0.030, 0.045, 0.060, 0.075, and 0.090 mM) of compounds and Trolox (Sigma-Aldrich; dissolved in DMSO) were used. The percent inhibition was calculated according to

the measured absorbance (% Inhibition = $(A_0–A)/A_0$, where A_0 is absorbance of the supernatant of cell lysates) and was plotted as a function of compound concentration. The TEAC value of ligands was calculated as a ratio of the slope of the standard curve of the compound to that of Trolox. The measurements were conducted in triplicate.

2.4.3. Cell Viability Studies. The N2a and M17 neuroblastoma cell lines were purchased from ATCC. For the M17 cell line, 50% minimum essential medium (MEM) and 50% F12 were added instead of 50% DMEM, 50% OPTI-MEM, and 1% non-essential amino acids (NEAA, GIBCO). The cells were grown and maintained at 37 °C in a humidified atmosphere with 5% CO_2. Cell viability upon treatment of compounds was determined using the MTT assay (Sigma). Cells were seeded in a 96 well plate (15,000 cells in 100 μL per well). The N2a and M17 cells were treated with or without Aβ and $CuCl_2$ or $ZnCl_2$, followed by the addition of compounds (1% v/v final DMSO concentration) and incubated for 24 h. After incubation, 25 μL MTT [5 mg/mL in phosphate buffered saline (PBS), pH 7.4, GIBCO, Grand Island, NY, USA] was added to each well and the plate was incubated for 4 h at 37 °C. Formazan produced by the cells was solubilized using an acidic solution of *N*,*N*-dimethylformamide (50%, v/v aq) and sodium dodecyl sulfate (SDS, 20%, w/v) overnight at room temperature in the dark. The absorbance was measured at 600 nm using a microplate reader. Cell viability was calculated relative to cells containing an equivalent amount of DMSO.

2.5. References

(1) Rauk, A. *Chem. Soc. Rev.* **2009**, *38*, 2698–2715.

(2) Kepp, K. P. *Chem. Rev.* **2012**, *112*, 5193–5239.

(3) Faller, P.; Hureau, C.; Berthoumieu, O. *Inorg. Chem.* **2013**, *52*, 12193–12206.

(4) DeToma, A. S.; Salamekh, S.; Ramamoorthy, A.; Lim, M. H. *Chem. Soc. Rev.* **2012**, *41*, 608–621.

(5) Wang, Y. J.; Zhou, H. D.; Zhou, X. F. *Drug Discov. Today* **2006**, *11*, 931–938.

(6) Bharadwaj, P. R.; Dubey, A. K.; Masters, C. L.; Martins, R. N.; Macreadie, I. G. *J. C ell. Mol. Med.* **2009**, *13*, 412–421.

(7) Lee, S.; Fernandez, E. J.; Good, T. A. *Protein sci.* **2007**, *16*, 723–732.

(8) Savelieff, M. G.; Lee, S.; Liu, Y.; Lim, M. H. *ACS Chem. Biol.* **2013**, *8*, 856–865.

(9) Lee, S.; Zheng, X.; Krishnamoorthy, J.; Savelieff, M. G.; Park, H. M.; Brender, J. R.; Kim, J. H.; Derrick, J. S.; Kochi, A.; Lee, H. J.; Kim, C.; Ramamoorthy, A.; Bowers, M. T.; Lim, M. H. *J. Am. Chem. Soc.* **2014**, *136*, 299–310.

(10) Rival, T.; Page, R. M.; Chandraratna, D. S.; Sendall, T. J.; Ryder, E.; Liu, B.; Lewis, H.; Rosahl, T.; Hider, R.; Camargo, L. M.; Shearman, M. S.; Crowther, D. C.; Lomas,

D. A. *Eur. J. Neurosci.* **2009**, *29*, 1335–1347.

(11) Zhao, Y.; Zhao, B. *Oxid. Med. Cell. Longev.* **2013**, *2013*, 316523–316532.

(12) Tougu, V.; Tiiman, A.; Palumaa, P. *Metallomics* **2011**, *3*, 250–261.

(13) Choi, J. S.; Braymer, J. J.; Nanga, R. P.; Ramamoorthy, A.; Lim, M. H., *Proc. Natl. Acad. Sci. U. S. A.* **2010**, *107*, 21990-21995.

(14) Kung, H. F.; Lee, C. W.; Zhuang, Z. P.; Kung, M. P.; Hou, C.; Plossl, K. *J. Am. Che m. Soc.* **2001**, *123*, 12740–12741.

(15) Wang, C. C.; Chu, C. Y.; Chu, K. O.; Choy, K. W.; Khaw, K. S.; Rogers, M. S.; Pan g, C. P. *Clin. Chem.* **2004**, *50*, 952–954.

(16) Re, R.; Pellegrini, N.; Proteggente, A.; Pannala, A.; Yang, M.; Rice-Evans, C. *Free Ra dic. Biol. Med*. **1999**, *26*, 1231–1237.

(17) Miller, N. J.; Rice-Evans, C. A. *Free Radic. Res.* **1997**, *26*, 195–199.

(18) Schugar, H.; Green, D. E.; Bowen, M. L.; Scott, L. E.; Storr, T.; Bo hmerle, K.; Tho mas, F.; Allen, D. D.; Lockman, P. R.; Merkel, M.; Thompson, K. H.; Orvig, C. *Ange w. Chem., Int. Ed.* **2007**, *46*, 1716−1718.

(19) Spencer, V. A.; Sun, J. M.; Li, L.; Davie, J. R. *Methods* **2003**, *31*, 67–75.

Chapter 3. Investigations on Biochemical Activity of the Glycosylated Polyphenols and Their Esterified Derivatives toward Alzheimer's Disease

3.1. Introduction

Alzheimer's disease (AD) is a growing concern for the global public health as the most desperate neurological disorder by the absence of fundamental treatments or cures for the disease.[1] While numerous potential therapeutics have been developed for AD, their clinical success and a rational discovery of the drugs are still limited due to unidentified causes and the lack of understanding of the disease progression.[2,3,6] AD is a form of the protein misfolding diseases (called amyloidosis), characterized by the observation of the cellular deposits of the fibrillar peptide, senile plaques, and of the intraneuronal fibrillar tangles in the brain, composed primarily of amyloid-β (both the $A\beta_{40}$ and $A\beta_{42}$ isoforms) and hyperphosphorylated tau protein, respectively.[4-6]

The senile plaques found in the AD-affiliated brain have been shown to contain abnormally concentrated transition metals, Cu(I/II), Zn(II), and Fe(II/III). Especially, Zn(II) and Cu(II) have been proposed to accelerate the aggregation of Aβ forming a variety of nonfibrillar aggregates along the aggregation pathway.[7,8] Additionally, the interaction of Aβ with redox active metals like Cu(I/II) and Fe(II/III) could facilitate the production of reactive oxygen species (ROS) *via* Fenton-like reactions, which promotes oxidative stress in the diseased brain.[9,10,13] The potential interconnection of Aβ, metals, and ROS on the AD pathogenesis makes it difficult to characterize causes and their influence on the disease onset and progression. Small molecules targeting a variety of metal–Aβ that have been proposed as an interconnector of multiple factors (*e.g.*, Aβ, metals, metal–Aβ, ROS) have been developed either through rational design or screening of natural products.[11,12] Additionally, given the observations on the increase in oxidative stress found in the AD-affected brain, compounds with antioxidant capacity could also be beneficial.[6,13] Herein, natural polyphenolic glycosides (**Phlorizin**, **Verbascoside**, and **Rutin**) and their esterifed derivatives (**F2**, **VPP**, and **R2**, respectively) were selected and investigated in terms of metal binding property, antioxidant capacity and inhibitory activity toward cytotoxicity induced by metal–Aβ.

3.2. Results and Discussion

3.2.1. Design Consideration of Glycosylated Polyphenols and Their Esterified Derivatives. In order to develop natural small molecules that could target metal–Aβ species, polyphenolic compounds, **Phlorizin**, **Verbascoside**, and **Rutin** were selected based on the previous reports (Figure 3.1).[14-19] Polyphenolic compounds have been shown to have potential antiamyloidogenic activity.[14,15] Both **Verbascoside** and **Rutin** have previously demonstrated the potential to redirect Aβ aggregation toward nontoxic species,[16-19] and **phloretin**, the nonglycosidic version of **Phlorizin,** has demonstrated

an ability to prevent membrane-associated aggregation of Aβ.[29] These preliminary studies examined aggregation in the absence of metal ions; thus the presence of known metal interaction moieties, phenol in **Phlorizin** and catechol in **Verbascoside** and **Rutin**, suggests that these compounds may be capable of simultaneously interacting with both Aβ and metals.[30,31] Moerover, all three compounds are known as antioxidants. In addition to three natural products, their derivatives, **F2, VPP**, and **R2** were designed *via* selective esterification (Figure 3.1, orange).[20,21] Esterification could provide many structural and functional benefits in the quest for an effective chemical tool toward metal–Aβ. Ester formation of the compounds is in part employed to protect their functionality and enhance targeted delivery and which is primarily programed to release the proto-compound *via* enzymatic cleavage of ester groups within the cell.[22] In addition, the introduction of alkyl groups during the esterification may improve the ability of the compounds to passively diffuse across the blood brain barrier (BBB) due to improved lipophilicity.[12,23] Finally, the concomitant increase in the hydrophobicity of the compounds might give them better chance to act with Aβ/metal–Aβ species *via* a nonpolar interaction.[6,24]

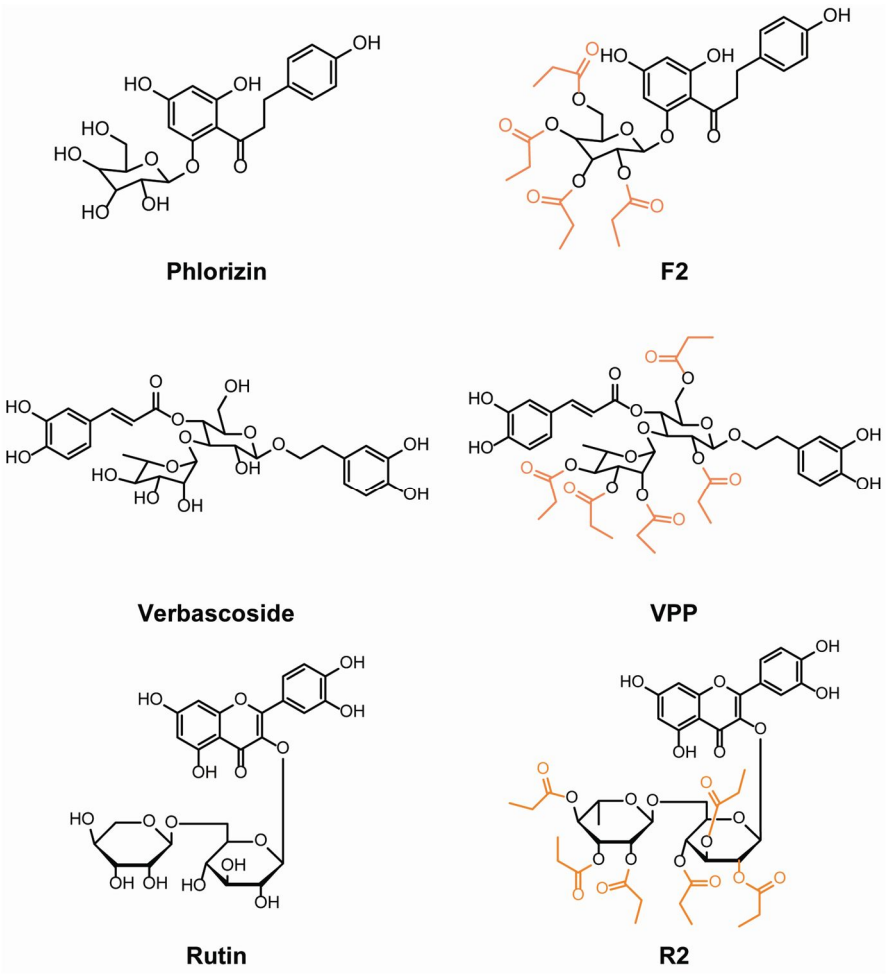

Figure 3.1. Chemical structures of glycosylated polyphenols and their derivatives. **Phlorizin**, 1-(2,4-

dihydroxy-6-(((2*S*,3*R*,4*R*,6*R*)-3,4,5-trihydroxy-6-(hydroxymethyl)tetrahydro-2*H*-pyran-2-yl)oxy)phenyl)-3-(4-hydroxyphenyl)propan-1-one; **Verbascoside**, (2*R*,3*R*,4*R*,5*R*,6*R*)-6-(3,4-dihydroxy phenethoxy)-5-hydroxy-2-(hydroxymethyl)-4-(((2*S*,3*R*,4*R*,5*R*)-3,4,5-trihydroxy-6-methyltetrahydro-2*H*-pyran-2-yl)oxy)tetrahydro-2*H*-pyran-3-yl(*E*)-3-(3,4-dihydroxyphenyl)-acrylate; **Rutin**, 2-(3,4-dihydroxy phenyl)-5,7-dihydroxy-3-(((2*S*,3*R*,4*S*,5*S*,6*R*)-3,4,5-trihydroxy-6-((((2*S*,3*R*,4*R*,5*S*)-3,4,5-trihydroxyl-tetrahydro-2*H*-pyran-2-yl)oxy)methyl)tetrahydro-2*H*-pyran-2-yl)oxy)-4*H*-chromen-4-one; **F2**, (2*S*,3*R*,4*R*,6*R*)-2-(3,5-dihydroxy-2-(3-(4-hydroxyphenyl)pro-panoyl)phenoxy)-6-((propionyloxy) methyl)tetrahydro-2*H*-pyran-3,4,5-triyl tripropionate; **VPP**, (2*S*,3*R*,4*R*,5*S*)-2-(((2*R*,3*R*,4*S*,5*R*,6*R*)-2-(3,4-dihydroxyphenethoxy)-5-(((*E*)-3-(3,4-dihydroxyphenyl)acryloyl)oxy)-3-(propionyloxy)-6-((propionyloxy)methyl)tetrahydro-2*H*-pyran-4-yl)oxy)-6-methyltetrahydro-2*H*-pyran-3,4,5-triyl tripropionate; **R2**, (2*R*,3*R*,4*R*,5*S*,6*S*)-2-(((2*R*,3*R*,4*S*,5*R*,6*S*)-6-((2-(3,4-dihydroxyphenyl)-5,7-dihydroxy-4-oxo-4*H*-chromen-3-yl)oxy)-3,4,5-tris(propionyloxy)tetrahydro-2*H*-pyran-2-yl)methoxy)-6-methyltetrahydro-2*H*-pyran-3,4,5-triyl tripropionate.

3.2.2. Metal Binding Properties of Polyphenols. In order to understand the interaction of the compounds with metal ions, particularly Cu(II) and Zn(II), their metal binding properties are investigated by visible spectroscopy (UV−vis) or 1D ^{1}H NMR. Cu(II) binding of **Phlorizin**/**F2**, **Verbascoside**/**VPP**, or **Rutin**/**R2** was investigated using UV−vis; Zn(II) binding of **Verbascoside** and **VPP** were studied by ^{1}H NMR due to a lack of significant optical changes in the spectra upon addition of $ZnCl_2$. In the buffered aqueous solution (20 μM HEPES, pH 7.4), it was observed that the absorption spectra of the six polyphenols changed to different extents upon the titration of $CuCl_2$ (Figure 3.2). Addition of $CuCl_2$ to solutions of either **Phlorizin** or **F2** produced no significant shift in spectral features, possibly due to the weak affinity of the phenol moiety in both compounds for Cu(II) in solution (Figure 3.2). **F2** showed a decrease in the overall spectral intensity upon titration of $CuCl_2$; this may be the result of breakdown or oxidation catalyzed by the presence of Cu(II) in solution.[28] This tendency of **Phlorizin** and **F2** may be understood as recognition of the absence of the catechol functionality in their structure. In contrary, titration of $CuCl_2$ to both **Verbascoside** and **VPP** in solution induced a slight variation on the absorption bands at *ca*. 330 nm and 405 nm, suggesting potential interaction between both ligands and Cu(II) under this condition (Figure 3.2). The spectral change is found more dramatic in **VPP** than in **Verbascoside**, which suggests that esterification contributes on the Cu(II) interaction property of the compounds even though this chemical modification is directed to the peripheral sites of the proposed metal binding portion. The presence of Cu(II) did induce modest spectral changes in the spectrum of **Rutin** (Figure 3.2) causing a decrease in the primary peak *ca*. 330 nm and an increase in a shoulder *ca*. 425 nm upon addition of $CuCl_2$. This likely is the result of the interaction between the catechol moiety and Cu(II).[15,27] Finally, **R2** demonstrated minimal spectral change over the course of the titration, suggesting it has minimal or no interaction with Cu(II) (Figure 3.2). This suggests that esterification of the **Rutin** framework could change the interaction between the ligand and Cu(II). Both **VPP** and **R2** were esterified from their parent compounds but the extent of change in Cu-induced spectral variation was different, which may indicate importance of overall structure on the metal binding property of the compounds.

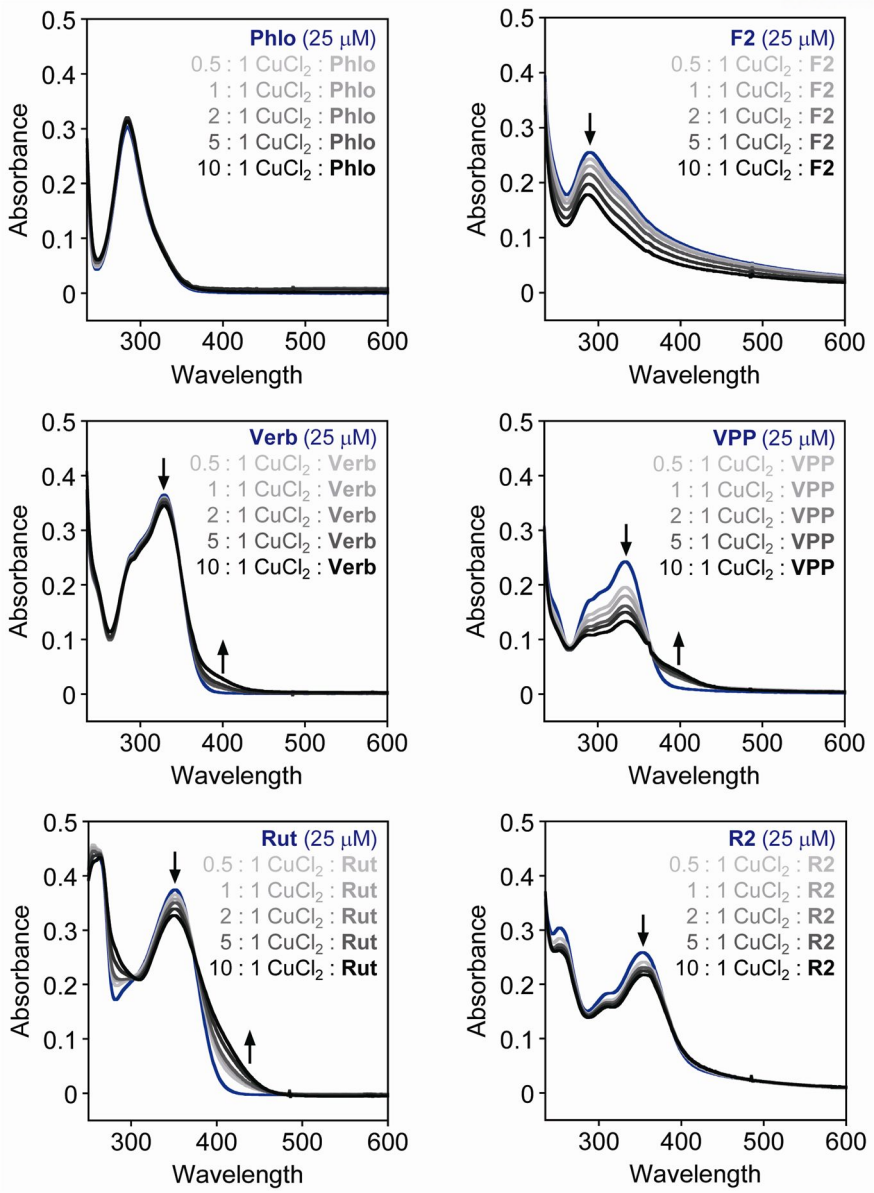

Figure 3.2. Cu(II) binding studies of **Phlorizin**, **F2**, **Verbascoside**, **VPP**, **Rutin**, and **R2** observed by UV−vis. Samples were incubated for 2 h with and without Cu(II) (0.5−10 equiv) at pH 7.4 at room temperature.

The interaction between **Verbascoside** and **VPP** with Zn(II) in DMSO-d_6 was investigated by ^{1}H NMR. After the addition of 2 equiv $ZnCl_2$ to the solution, significant sharpening of all protons of the catechol OH groups was observed (Figure 3.3): Note that the assignment of individual signals of these protons is difficult to predict from our 1D NMR data.[32] Peak sharpening may be due to an increased tumbling of these protons because the catechol OH group could have better solvation upon interaction with Zn(II). Overall, the results suggest that **Verbascoside**, **VPP**, **Rutin**, and **R2** could potentially interact to Cu(II) and/or Zn(II) while **Phlorizin** and **F2** did not as evidenced by metal-induced UV-vis spectral shift of the ligands, which indicates the necessity of catechol moiety to interact with metal ions.

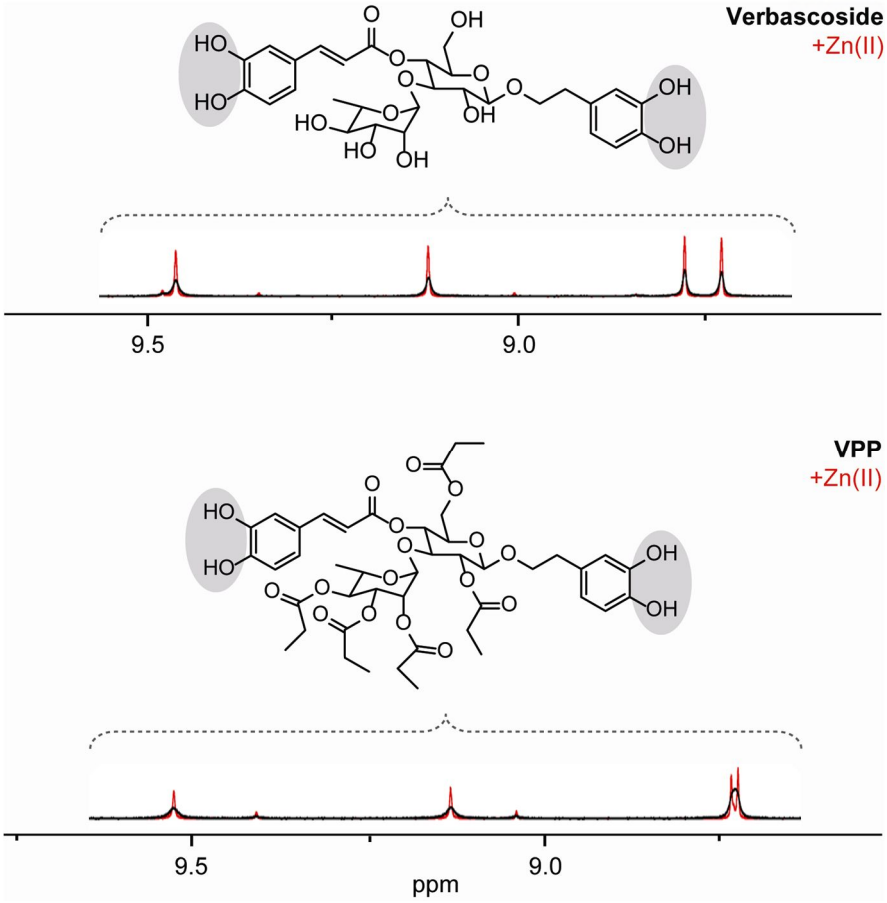

Figure 3.3. Zn(II) binding of **Verbascoside** and **VPP** observed by ^{1}H NMR. Samples were incubated for 30 min with $ZnCl_2$ (0 or 2 equiv) in DMSO-d_6 at room temperature.

3.2.3. Antioxidant Properties. The ability of these six polyphenols to scavenge free radicals [the ABTS cation radical ($ABTS^{\bullet+}$); ABTS = 2,2'-azino-bis(3-ethylbenzothiazoline-6-sulfonic acid)] was probed by the Trolox equivalence antioxidant capacity (TEAC) assay using cell lysates (Figure 3.4).[25,26] Both **Verbascoside** and **Rutin**, two known antioxidants,[30,32] scavenged $ABTS^{\bullet+}$ marginally better than Trolox (by a factor of *ca*. 2.0 and 1.5, respectively). **VPP** and **Phlorizin** showed a slightly lower ability to scavenge $ABTS^{\bullet+}$ relative to Trolox. **R2** and **F2**, meanwhile, indicated a lower TEAC value than Trolox, suggesting a limited function as an antioxidant relative to the other compounds investigated herein. This, again, indicates that esterification of the sugar moiety alters the function of the **Verbascoside** framework. In this case, the antioxidant capacity of the framework was reduced by *ca*. 40% following esterification. This reduction in antioxidant capacity is surprising given the conservation of the catechol structures between **Verbascoside** and **VPP** which is thought to be potentially responsible for $ABTS^{\bullet+}$ quenching through semi-quinone and quinone formation.[26,27]

3.2.4. Regulating Toxicity Induced by Metal-Free and Metal-Associated Aβ in Living Cells. In the previous studies, **Verbascoside** and **Rutin** have been suggested to alleviate the toxicity of metal-

free Aβ species.[17,19] We have probed this relationship further to examine the effect of these two compounds and **VPP** on the toxicity triggered by both metal-free Aβ and metal–Aβ in murine Neuro-2a (N2a) neuroblastoma cells. Upon addition of **Verbascoside** (5–25 μM), cell viability was increased in both metal-free and metal-treated cells (*ca*. 90–100% cell survival; Figure 3.5a). In the case of esterified **VPP** (5–10 μM), the treatment with this compound (5–10 μM) presented approximately 90% cell survival without and with metal ions and showed *ca*. 70% decreased viability at 25 μM in the presence of either Cu(II) or Zn(II) (Figure 3.5a). In addition, **Rutin** indicated no significant impact on cell viability under any conditions (Figure 3.5a).

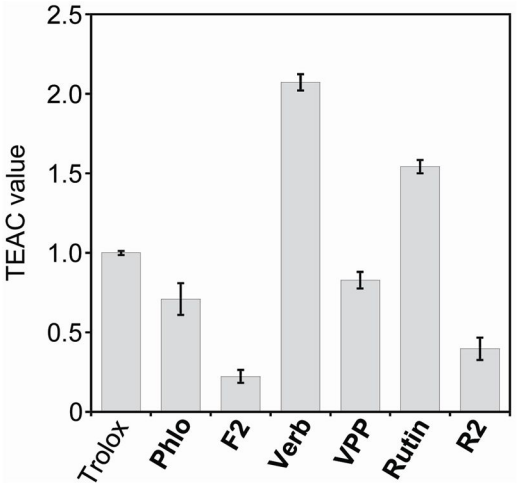

Figure 3.4. Antioxidant activity of **Phlorizin**, **F2**, **Verbascoside**, **VPP**, **Rutin**, and **R2** evaluated by the cell lysate-based TEAC assay. The TEAC values are relative to a vitamin E analogue, Trolox (6-hydroxy-2,5,7,8-tetramethylchroman-2-carboxylic acid).

The ability of **Verbascoside**, **VPP**, and **Rutin** to mitigate cytotoxicity induced by metal-free and metal–Aβ was also investigated. Cells incubated with Aβ (20 μM) with or without metal ions [Cu(II) or Zn(II); 20 μM] showed *ca*. 70–80% viability under all conditions (Figure 3.5b). The addition of **Verbascoside** (20 μM) to the cells preincubated with Aβ in both the absence and presence of metal ions significantly improved cell viability (*ca*. 90–100%). **VPP** (20 μM), however, was generally unable to regulate cytotoxicity of the various Aβ species; in the absence and presence of Cu(II), **VPP** decreased cell viability to levels lower than Cu(II)–Aβ. Finally, the treatment of cells with **Rutin** (20 μM) minimally improved cell viability under all conditions. Overall, only **Verbascoside** is capable of attenuating the broad toxicity of both Aβ and metal–Aβ. Furthermore, esterification of this framework limited this observed regulatory activity toward Aβ and metal–Aβ in living cells.

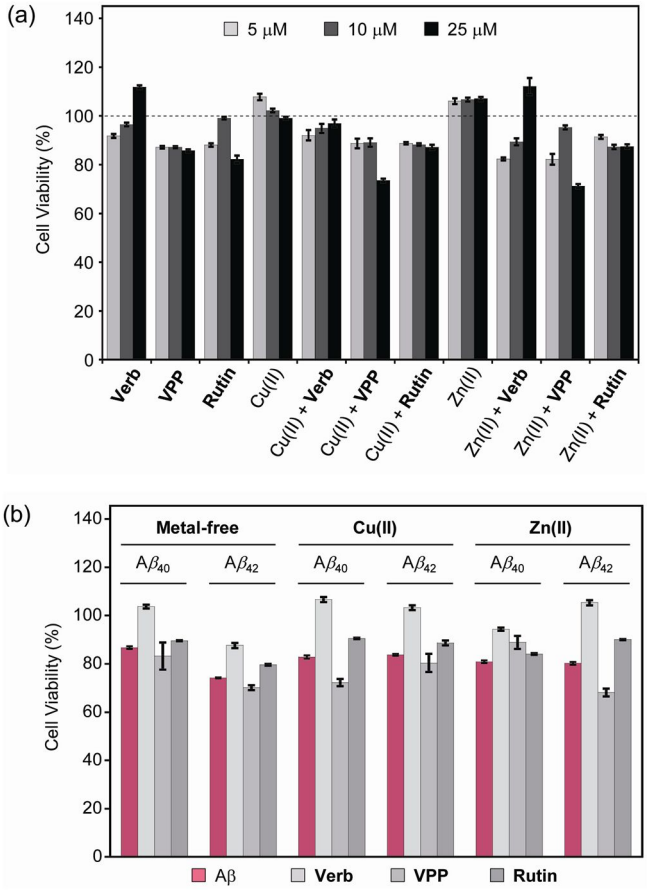

Figure 3.5. Influence of **Verbascoside**, **VPP**, and **Rutin** on toxicity induced by Aβ or metal–Aβ in murine Neuro-2a neuroblastoma (N2a) cells. (a) Cytotoxicity of compounds with or without metal ions. Cells treated with compounds [**Verbascoside**, **VPP**, and **Rutin** (5–25 μM)] with or without various concentrations of a metal chloride salt ($CuCl_2$ or $ZnCl_2$; 5–25 μM) were incubated for 24 h at 37 °C. (b) Influence of **Verbascoside**, **VPP**, and **Rutin** on cytotoxicity induced by metal-free Aβ and metal–Aβ species in N2a cells. Cells treated with $Aβ_{40}$/$Aβ_{42}$ (20 μM), a metal chloride salt ($CuCl_2$ or $ZnCl_2$; 20 μM), and a compound (**Verbascoside**, **VPP**, or **Rutin**; 20 μM) were incubated for 24 h at 37 °C. Cell viability was determined by the MTT assay. The values of viability (%) were calculated compared to cells treated with DMSO only (0–1%, v/v). Error bars represent the standard error from three independent experiments.

3.3. Conclusion

The natural glycosylated polyphenols, **Phlorizin**, **Verbascoside**, and **Rutin**, along with their esterified derivatives, **F2**, **VPP**, and **R2**, were investigated for their potential to target multiple factors (*e.g.*, Aβ, metals, metal–Aβ, free radicals) and modulate their reactivities. UV–vis and NMR studies demonstrated that both **Verbascoside** and **VPP** having catechol moieties are able to interact with Cu(II) and Zn(II). In addition, **Verbascoside** is shown to have an antioxidant capacity and no toxicity up to the concentration tested. Overall, our studies suggest **Verbascoside** as a promising framework for a multifunctional chemical reagent to interrogate the etiology of AD. In addition, synthetic derivatization of parent scaffolds showing functionality should be carefully carried out in order to maintain or improve their functions.

3.4. Experimental Sections

3.4.1. Metal Binding Studies. The interactions of **Phlorizin**, **F2**, **Verbascoside**, **VPP**, **Rutin**, and **R2** with Cu(II) and Zn(II) were determined by UV-vis or ^{1}H NMR. A solution of ligands (25 μM in HEPES, pH 7.4, 150 μM NaCl) was prepared, treated with 0.5 to 10 equiv of $CuCl_2$, and incubated at room temperature for 2 h (for **Phlorizin**, **F2**, **Verbascoside**, **VPP**, **Rutin**, and **R2**). The optical spectra of the resulting solutions were measured by UV–vis. The interaction of **Verbascoside** or **VPP** with $ZnCl_2$ was observed by ^{1}H NMR (400 MHz). One equiv of $ZnCl_2$ was added to a solution of **Verbascoside** or **VPP** (2 mM) in DMSO-d_6; the resulting spectral shifts were recorded.

3.4.2. Trolox Equivalent Antioxidant Capacity (TEAC) Assay. The antioxidant activity of **Phlorizin**, **F2**, **Verbascoside**, **VPP**, **Rutin**, and **R2** was determined by the TEAC assay employing cell lysates following the protocol of the antioxidant assay kit purchased from Cayman Chemical Company (Ann Arbor, MI, USA) with modifications.[33,34] The murine Neuro-2a (N2a) cells were used for this assay. This cell line purchased from the American Type Culture Collection (ATCC, Manassas, VA, USA) was maintained in media containing 50% Dulbecco's modified Eagle's medium (DMEM) and 50% OPTI-MEM (GIBCO), supplemented with 10% fetal bovine serum (FBS, Sigma), 1% Non-essential Amino Acids (NEAA, GIBCO), 2 mM glutamine, 100 U/ml penicillin, and 100 mg/ml streptomycin (GIBCO). The cells were grown and maintained at 37 °C in a humidified atmosphere with 5% CO_2. For the antioxidant assay using cell lysates, cells were seeded in a 6 well plate and grown to approximately 80–90% confluence. Cell lysates were prepared following the previously reported method with modifications.[35] N2a cells were washed once with cold PBS (pH 7.4, GIBCO) and harvested by gently pipetting off adherent cells with cold PBS. The cell pellet was generated by centrifugation (2,000 x g for 10 min at 4 °C). This cell pellet was sonicated on ice (5 sec pulses, 5 times with 20 sec intervals between each pulse) in 2 mL of cold Assay Buffer (5 mM potassium phosphate, pH 7.4, containing 0.9% NaCl and 0.1% glucose). The cell lysates were centrifuged at 5,000 x g for 10 min at 4 °C. The supernatant was removed and stored on ice until use. To standard and sample 96 wells, 10 μL of the supernatant of cell lysates was delivered followed by addition of compound, metmyoglobin, ABTS, and hydrogen peroxide in order. After 5 min incubation at room temperature on a shaker, absorbance values at 750 nm were recorded. The final concentrations (0.015, 0.030, 0.045, 0.060, 0.075, and 0.090 mM) of **Phlorizin**, **F2**, **Verbascoside**, **VPP**, **Rutin**, **R2** and Trolox (Sigma-Aldrich; Trolox = 6-hydroxy-2,5,7,8-tetramethylchroman-2-carboxylic acid; dissolved in DMSO) were used. The percent inhibition was calculated according to the measured absorbance (% Inhibition = $(A_0–A)/A_0$, where A_0 is absorbance of the supernatant of cell lysates) and was plotted as a function of compound concentration. The TEAC value of ligands was calculated as a ratio of the slope of the standard curve of the compound to that of Trolox.

3.4.3. Cell Viability Studies. The N2a cell line was purchased from ATCC. The cells were grown and maintained at 37 °C in a humidified atmosphere with 5% CO_2. Cell viability upon treatment of compounds was determined using the MTT assay (Sigma). N2a cells were seeded in a 96 well plate (15,000 cells in 100 μL per well). The cells were treated with or without Aβ and $CuCl_2$ or $ZnCl_2$, followed by the addition of compounds (1% v/v final DMSO concentration for **Verbascoside**, **VPP**, and **Rutin**) and incubated for 24 h in the cells. After incubation, 25 μL MTT [5 mg/mL in phosphate buffered saline (PBS), pH 7.4, GIBCO, Grand Island, NY, USA] was added to each well and the plate was incubated for 4 h at 37 °C. Formazan produced by the cells was solubilized using an acidic solution of *N*,*N*-dimethylformamide (DMF, 50%, v/v aq) and sodium dodecyl sulfate (SDS, 20%, w/v) overnight at room temperature in the dark. The absorbance was measured at 600 nm using a microplate reader. Cell viability was calculated relative to cells containing an equivalent amount of DMSO.

3.5. References

(1) Jakob-Roetne, R.; Jacobsen, H., *Angew. Chem. Int. Ed. Engl.* **2009**, *48*, 3030–3059.

(2) Gouras, G. K.; Olsson, T. T.; Hansson, O., *Neurotherapeutics* **2014**, http://dx.doi.org/10.1007/s13311-014-0313-y.

(3) Franco, R.; Cedazo-Minguez, A., *Front. Pharmacol.* **2014**, *5*, 146–158.

(4) Rauk, A. *Chem. Soc. Rev.* **2009**, *38*, 2698–2715.

(5) Hamley, I. W. *Chem. Rev.* **2012**, *112*, 5147–5192.

(6) Savelieff, M. G.; Lee, S.; Liu, Y.; Lim, M. H. *ACS Chem. Biol.* **2013**, *8*, 856–865.

(7) Kepp, K. P. *Chem. Rev.* **2012**, *112*, 5193–5239.

(8) Faller, P.; Hureau, C.; Berthoumieu, O. *Inorg. Chem.* **2013**, *52*, 12193–12206.

(9) Parthasarathy, S.; Yoo, B.; McElheny, D.; Tay, W.; Ishii, Y. *J. Biol. Chem.* **2014**, *289*, 9998–10010.

(10) Eskici, G.; Axelsen, P. H. *Biochemistry* **2012**, *51*, 6289–6311.

(11) Savelieff, M. G.; DeToma, A. S.; Derrick, J. S.; Lim, M. H. *Acc. Chem. Res.* **2014**, *47*, 2475–2482.

(12) Beck, M. W.; Pithadia, A. S.; DeToma, A. S.; Korshavn, K. J.; Lim, M. H., Ligand Design to Target and Modulate Metal-Protein Interactions in Neurodegenerative Diseases. *Ligand Design in Medicinal Inorganic Chemistry*, Storr, T., Ed. John Wiley & Sons, Ltd. Chinchester, West Sussex, United Kingdom, **2014**; pp 257–286.

(13) Faller, P.; Hureau, C. *Chemistry* **2012**, *18*, 15910–15920.

(14) Porat, Y.; Abramowitz, A.; Gazit, E. *Chem. Biol. Drug Des.* **2006**, *67*, 27–37.

(15) Hyung, S. J.; DeToma, A. S.; Brender, J. R.; Lee, S.; Vivekanandan, S.; Kochi, A.; Choi, J. S.;

Ramamoorthy, A.; Ruotolo, B. T.; Lim, M. H. *Proc Natl. Acad. Sci. U. S. A.* **2013**, *110*, 3743–3748.

(16) Kurisu, M.; Miyamae, Y.; Murakami, K.; Han, J.; Isoda, H.; Irie, K.; Shigemori, H. *Biosci. Biotechnol. Biochem.* **2013**, *77*, 1329–1332.

(17) Wang, H.; Xu, Y.; Yan, J.; Zhao, X.; Sun, X.; Zhang, Y.; Guo, J.; Zhu, C. *Brain. Res.* **2009**, *1283*, 139–147.

(18) Wang, S. W.; Wang, Y. J.; Su, Y. J.; Zhou, W. W.; Yang, S. G.; Zhang, R.; Zhao, M.; Li, Y. N.; Zhang, Z. P.; Zhan, D. W.; Liu, R. T. *Neurotoxicology* **2012**, *33*, 482–490.

(19) Jimenez-Aliaga, K.; Bermejo-Bescos, P.; Benedi, J.; Martin-Aragon, S. *Life Sci.* **2011**, *89*, 939–945.

(20) Baldisserotto, A.; Malisardi, G.; Scalambra, E.; Andreotti, E.; Romagnoli, C.; Vicentini, C. B.; Manfredini, S.; Vertuani, S. *Molecules* **2012**, *17*, 13275–13289.

(21) Vertuani, S.; Beghelli, E.; Scalambra, E.; Malisardi, G.; Copetti, S.; Dal Toso, R.; Baldisserotto, A.; Manfredini, S. *Molecules* **2011**, *16*, 7068–7080.

(22) Rautio, J.; Kumpulainen, H.; Heimbach, T.; Oliyai, R.; Oh, D.; Jarvinen, T.; Savolainen, J. *Nat. Rev. Drug. Discov.* **2008**, *7*, 255–270.

(23) Pardridge, W. M. *J. Cereb. Blood. Flow. Metab.* **2012**, *32*, 1959–1972.

(24) Nguyen, P.; Derreumaux, P. *Acc. Chem. Res.* **2014**, *47*, 603–611.

(25) Re, R.; Pellegrini, N.; Proteggente, A.; Pannala, A.; Yang, M.; Rice-Evans, C. *Free Radic. Biol. Med.* **1999**, *26*, 1231–1237.

(26) Rice-Evans, C. A.; Miller, N. J.; Paganga, G. *Free Radic. Biol. Med.* **1996**, *20*, 933–956.

(27) DeToma, A. S.; Krishnamoorthy, J.; Nam, Y.; Lee, H. J.; Brender, J. R.; Kochi, A.; Lee, D.; Onnis, V.; Congiu, C.; Manfredini, S.; Vertuani, S.; Balboni, G.; Ramamoorthy, A.; Lim, M. H. *Chem. Sci.* **2014**, *5*, 4851–4862.

(28) Oszmianski, J.; Lee, C. Y., *J. Agric. Food Chem.* **1991**, *39*, 1050–1052.

(29) Hertel, C.; Terzi, E.; Hauser, N.; Jakob-Rotne, R.; Seelig, J.; Kemp, J. A., *Proc. Natl. Acad. Sci. U. S. A.* **1997**, *94*, 9412–9416.

(30) Schweigert, N.; Zehnder, A. J.; Eggen, R. I., *Environ. Microbiol.* **2001**, *3*, 81–91.

(31) Severino, J. F.; Goodman, B. A.; Reichenauer, T. G.; Pirker, K. F., *Free Radic. Res.* **2011**, *45*, 115–124.

(32) Kontogianni, V. G.; Charisiadis, P.; Primikyri, A.; Pappas, C. G.; Exarchou, V.; Tzakos, A. G.; Gerothanassis, I. P., *Org. Biomol. Chem.* **2013**, *11*, 1013–1025

(33) Re, R.; Pellegrini, N.; Proteggente, A.; Pannala, A.; Yang, M.; Rice-Evans, C. *Free Ra dic. Biol. Med.* **1999**, *26*, 123̃11237.

(34) Schugar, H.; Green, D. E.; Bowen, M. L.; Scott, L. E.; Storr, T.; Bo hmerle, K.; Tho

mas, F.; Allen, D. D.; Lockman, P. R.; Merkel, M.; Thompson, K. H.; Orvig, C. *Angew. Chem., Int. Ed.* **2007**, *46*, 1716−1718.

(35) Spencer, V. A.; Sun, J. M.; Li, L.; Davie, J. R. *Methods* **2003**, *31*, 67−75.

Chapter 4. Investigations of Cytotoxicity Induced by the Human Islet Amyloid Polypeptide in the Absence and Presence of Metal Ions

4.1. Introduction

Type II diabetes mellitus (T2DM) is the most prevalent form of diabetes and characterized by a deficit pancreatic β cell induced by increased levels of circulating insulin to overcome insulin resistance.[1,2] The hallmark of type II diabetes is amyloid plaques composed of the human islet amyloid polypeptide (hIAPP) in pancreatic islets.[3,4] hIAPP is a 37 amino acid residue that is normally co-secreted with insulin by pancreatic β cells and involved in glucose metabolism.[4,5] hIAPP has the intrinsic propensity to self-associate to generate multiple conformations, *e.g.*, oligomers, protofibrils, and fibrils, and the previous *in vitro* studies report that these aggregated forms could cause toxicity to β cells and increase their apoptosis.[3,12] Furthermore, transition metal ions, such as Cu(II) and Zn(II), are suggested to be associated with the aggregation pathways of hIAPP; redox active metals [*i.e.*, Cu(I/II)]–hIAPP is proposed to produce reactive oxygen species (ROS) *via* Fenton-like reactions.[6,7] Although the interaction between metal ions and hIAPP has been observed, a relationship between this interaction and toxicity has not been fully revealed. In addition, which hIAPP species (*i.e.*, oligomers, fibers) cause cytotoxicity is still unclear.[8] Herein, to get a better understanding of toxicity induced by hIAPP, results from cytotoxicity studies are described: investigations of (i) metal influence on hIAPP's toxicity; (ii) hIAPP intermediates' toxicity; (iii) apoptosis induced by hIAPP in the absence and presence of metal ions.

4.2. Results and Discussion

4.2.1. Cytotoxicity of hIAPP in the Absence and Presence of Metal Ions. To investigate the cytotoxicity of hIAPP, rat insulinoma-1 (INS-1) pancreatic β cells were treated with hIAPP (10 or 20 μM) without and with metal ions ($CuCl_2$ or $ZnCl_2$, 70–140 μM) and the cell viability was measured by the MTT assay [MTT= 3-(4,5-dimethylthiazol-2-yl)-2,5-diphenyltetrazolium bromide] upon 24 h incubation. Cells treated with hIAPP in the absence of metal ions showed cell viability *ca*. 80% (Figure 4.1). The cells are treated with hIAPP (10 or 20 μM) and metal ions in a ratio of 1:7 peptide to metal. Upon addition of $CuCl_2$ (70 or 140 μM) to hIAPP-treated cells, cell viability was decreased by approximately 15% compared to that only with hIAPP (Figure 4.1). On the other hand, *ca*. 20% increased cell viability was observed when the cells were treated with hIAPP (10 μM) and $ZnCl_2$ (70 μM) while *ca*. 10% decreased viability was indicated upon treatment of cells with hIAPP (20 μM) and $ZnCl_2$ (140 μM), relative to that with hIAPP only (Figure 4.1). From the observation that Cu(II)–hIAPP-treated cells showed the lowest viability (*ca*. 60%) (Figure 4.1), further toxicity studies were carried out with variation of the ratio of hIAPP to Cu(II) (from 1:1 to 1:5) (Figure 4.2). *ca*. 75%

viability of cells treated with hIAPP only was observed; the cell survival was reduced down to *ca*. 55% as the ratio of hIAPP to Cu(II) was increased (Figure 4.2). Overall, hIAPP was indicated to have different toxicity in the absence and presence of metal ions, particularly showing altered toxicity of Cu(II)–hIAPP depending on peptide to metal ratios.

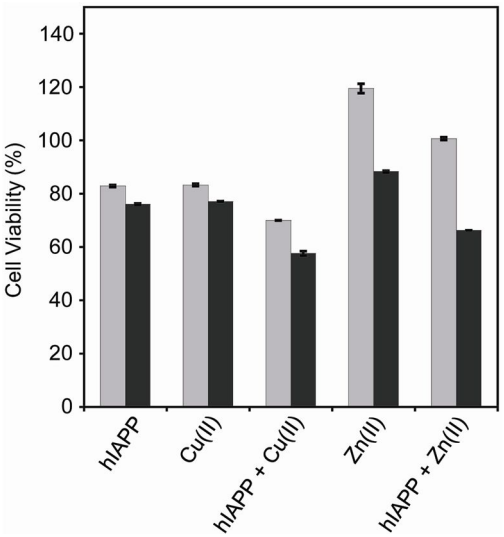

Figure 4.1. Cytotoxicity studies of the human islet amyloid polypeptide (hIAPP) in the rat insulinoma-1 (INS-1) pancreatic β cell. Cells were treated with hIAPP [10 μM (gray bars) or 20 μM (black bars)], with/without a metal chloride salt [$CuCl_2$ or $ZnCl_2$, 70 μM (gray bars) or 140 μM (black bars)] followed by 24 h incubation at 37 °C. The values of cell viability (%), measured by the MTT assay, were calculated compared to cells treated with H_2O only. Error bars represent the standard error from three independent experiments.

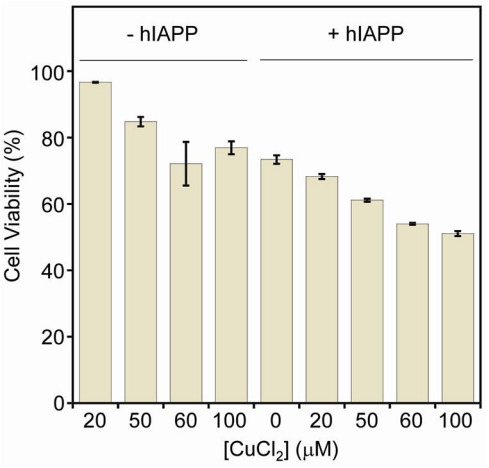

Figure 4.2. Cytotoxicity studies of the Cu(II)–hIAPP in the rat insulinoma-1 (INS-1) pancreatic β cell. Cells were treated with hIAPP (20 μM) without and with $CuCl_2$ (20–100 μM) and incubated for 24 h at 37 °C. The values of cell viability (%), measured by the MTT assay, were calculated compared to cells treated with H_2O only. Error bars represent the standard error from three independent experiments.

4.2.2. Peptide Conformation-Dependent Cytotoxicity. In order to investigate cytotoxicity of metal-

associated hIAPP species depending on the degree of their aggregation, INS-1 pancreatic β cells were treated with hIAPP that were preincubated with $CuCl_2$ or $ZnCl_2$ for different time periods (hIAPP, 10 or 20 μM; hIAPP:M(II) = 1:7; preincubation time: 1, 2, 3, or 9 h) followed by incubation for 6 h (Figure 4.3a) or 24 h (Figure 4.3b) at 37 °C. Viability of the cells added with preincubated hIAPP/metal–hIAPP was obtained by the MTT assay. Cells treated with preincubated samples for 6 h did not show noticeable variation to each other depending on the preincubation time points of hIAPP or metal–hIAPP (*ca*. 80–90% cell survival) (Figure 4.3a). On the other hand, cells with hIAPP preincubated with Cu(II) presented changes in their viability upon 24 h incubation depending on the preincubation time points (Figure 4.3b). The lowest cell viability was observed in the cells treated with hIAPP preincubated with Cu(II) for 3 h (*ca*. 60%) (Figure 4.3b). These overall results suggest that the aggregated hIAPP forms that were generated at 3 h incubation time point may be toxic living cells.

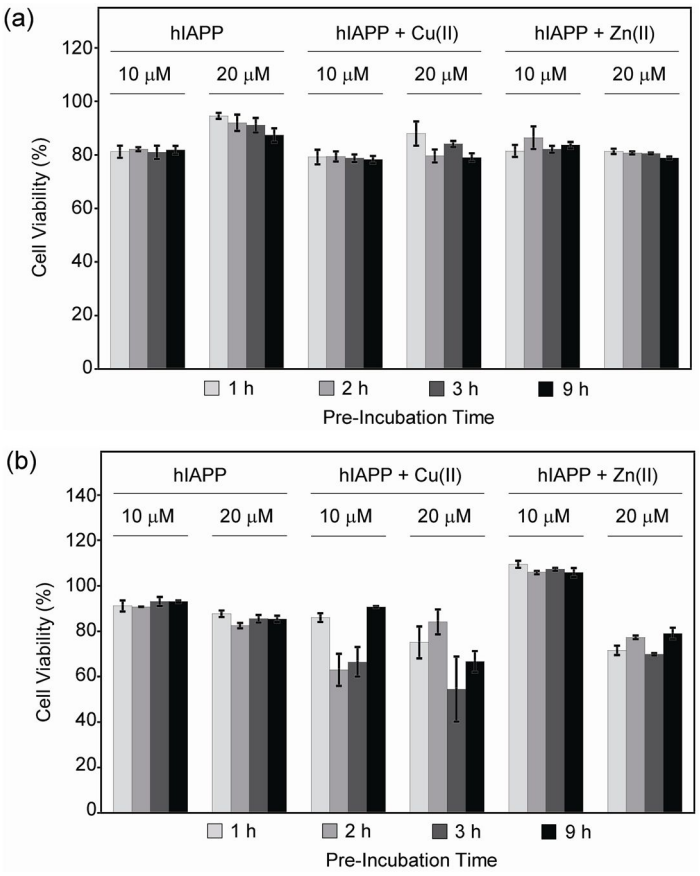

Figure 4.3. Cytotoxicity studies with hIAPP in the rat insulinoma-1 (INS-1) pancreatic β cell. Cell viability upon incubation time [(a) 6 h or (b) 24 h] after treatment with hIAPP and metal–hIAPP preincubated for 1 h, 2 h, 3 h, and 9 h. Cells were treated with samples incubated hIAPP (10–20 μM) without and with $CuCl_2$ or $ZnCl_2$ (70–140 μM) followed by 6 h or 24 h incubation at 37 °C. The values of cell viability (%), measured by the MTT assay after 24 h incubation, were calculated compared to cells treated with HEPES only. Error bars represent the standard error from three independent experiments.

In order to further investigate toxicity induced by metal–hIAPP, cytotoxicity studies were carried out with metal–hIAPP aggregates prepared after 3 h incubation [which indicated the lowest cell viability (Figure 4.3b)], upon varying metal ion concentrations. The INS-1 cells were treated with prepared metal–hIAPP (preincubated for 3 h; hIAPP, 20 μM; $CuCl_2$, 20–200 μM or $ZnCl_2$, 60–200 μM). In the case of Cu(II)–hIAPP, cell viability was proportionally reduced as a function of the concentration of $CuCl_2$ (Figure 4.4a). Different from Cu(II)–hIAPP, Zn(II)–hIAPP-treated cells exhibited no noticeable change in cell survival despite increasing the concentrations of $ZnCl_2$ (Figure 4.4b). Taken together, our results suggest that Cu(II)–hIAPP intermediates are potentially more toxic than Zn(II)-affiliated counterparts.

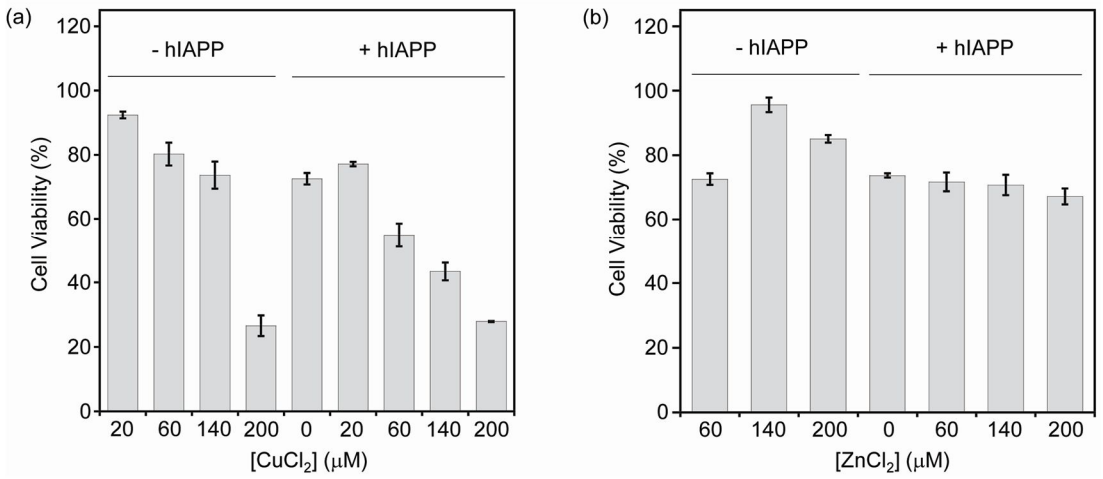

Figure 4.4. Cytotoxicity studies with the hIAPP in the rat insulinoma-1 (INS-1) pancreatic β cell. Cell viability upon treatment with metal-free hIAPP and metal–hIAPP preincubated for 3 h at 37 °C. Cells were treated with preincubated hIAPP (20 μM) with/without metal ions [(a) $CuCl_2$, 20–200 μM; (b) $ZnCl_2$, 60–200 μM] for 24 h incubation at 37 °C. The values of cell viability (%), obtained by the MTT assay, were calculated compared to cells treated with HEPES only. Error bars represent the standard error from three independent experiments.

4.2.3. Investigation of Apoptosis Induced by Metal-Free hIAPP or Metal–hIAPP. Previous studies have suggested that locally unstable membrane induced by toxic hIAPP oligomers cause cytoplasmic Ca(II) overproduction leading to endoplasmic reticulum (ER) stress and overactivation of Ca(II)-sensitive protease called calpain;[11] the cellular miscompartmentalization of Ca(II) could induce the β cell dysfunction and apoptosis in T2DM.[11,12] From these previous studies, it is reported that misfolded peptide species can be degraded by β cell autophagy;[13,14] thus its impairment may enhance cell death potentially *via* acceleration of hIAPP-induced β cell apoptosis.[13,14] To better understand a contribution of hIAPP-/Cu–hIAPP-induced apoptosis on the associated cellular failure, cytotoxicity studies were carried out against hIAPP-/metal–hIAPP-affiliated cells in the absence and presence of the known apoptosis inhibitor (calpain inhibitor, calpeptin,[11] or autophagy enhancer, trehalose[13,14]) or enhancer

(autophagy inhibitor, bafilomycin[13,14]).

Toxicity induced by hIAPP or Cu(II)–hIAPP was modulated upon addition of the compounds. Upon treatment with an inhibitor, calpeptin or trehalose, hIAPP-associated cells presented an increase in survival by approximately 10–20% in the absence and presence of Cu(II) in accordance with their inhibition property to different extents depending on their concentrations. These results indicate that mitigation of the toxicity may attribute to attenuation of hIAPP-/Cu(II)–hIAPP-associated apoptosis mediated by the inhibitors (Figures 4.5 and 4.6). Bafilomycin decreased cell viability with hIAPP and Cu(II)–hIAPP regardless of its concentrations (*ca*. 40–50%) (Figures 4.5 and 4.6). Thus, Calpeptin, trehalose, and bafilomycin displayed the ability to control β cell death induced by hIAPP with or without Cu(II); hIAPP-/Cu(II)–hIAPP-induced cytotoxicity was attenuated by calpeptin or trehalose and deteriorated by bafilomycin.

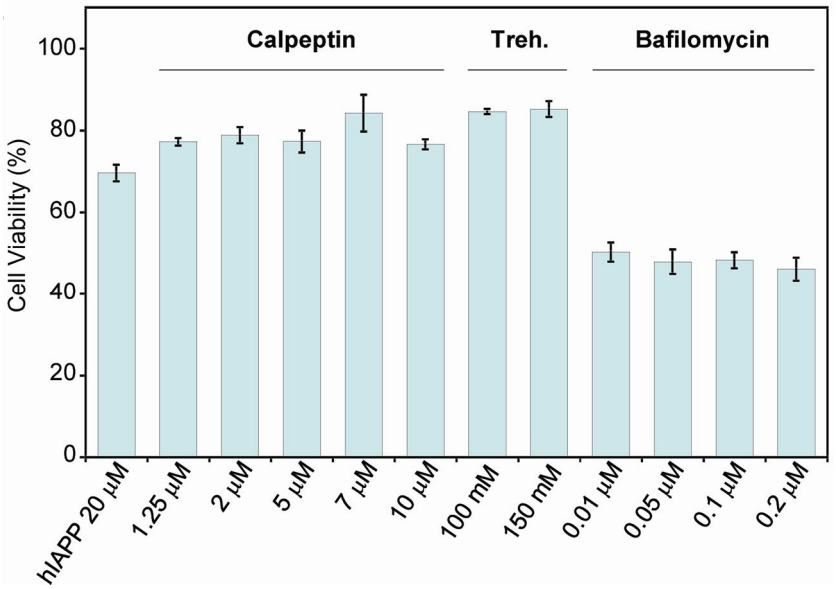

Figure 4.5. Cytotoxicity studies with the apoptosis reagents in the rat insulinoma-1 (INS-1) pancreatic β cell. Cell viability of hIAPP treated cells upon treatment of the apoptosis inhibitors (calpeptin or trehalose) or enhancer (bafilomycin) with various concentration of a compound. Condition: [hIAPP] = 20 μM; [calpeptin] = 1.25–10 μM, [trehalose] = 100–150 mM, [bafilomycin] = 0.01–0.2 μM; 24 h; 37 °C. The values of cell viability (%), obtained by the MTT assay, were calculated compared to cells treated with DMSO only (0–1%, v/v). Error bars represent the standard error from three independent experiments.

4.3. Conclusion

hIAPP is suggested to be a potential causative factor for the development of T2DM. Toxic intermediates of hIAPP can be generated during the abnormal aggregation process; however, several questions remain unclear: (i) how fibrillogenesis of hIAPP affects this disorder; (ii) how other factors (*i.e.*, metals) interact with hIAPP and influence its fibril formation and toxicity. To help these questions, the toxicity of hIAPP with and without metal ions under various conditions was

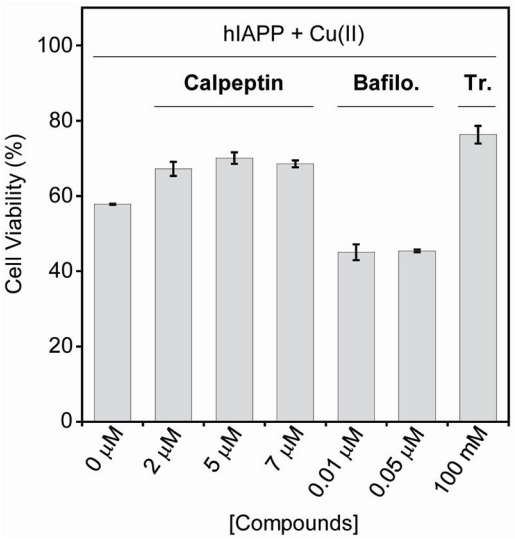

Figure 4.6. Cytotoxicity studies with the apoptosis reagents in the rat insulinoma-1 (INS-1) pancreatic β cell. Cells were treated with hIAPP (20 μM), with $CuCl_2$ (60 μM), and compounds (calpeptin, 2–7 μM; trehalose, 100 mM; bafilomycin, 0.01–0.05 μM) for 24 h at 37 °C. The values of cell viability (%), obtained by the MTT assay, were calculated compared to cells treated with DMSO only (0–1%, v/v). Error bars represent the standard error from three independent experiments.

investigated. From our studies, Cu(II)–hIAPP particularly, triggered an increase in cytotoxicity depending on metal concentration and intermediate formation generated at different incubation time periods. In addition, cytotoxicity mediated by hIAPP/metal–hIAPP was affected in the presence of an apoptosis inhibition (calpeptin or trehalose) or enhancer (bafilomycin).

4.4. Experimental Sections

4.4.1. Samples Preparation. hIAPP peptides were dissolved in 100% Hexafluoro-2-propanol (HFIP), aliquoted, lyophilized overnight, and stored at −80 °C. A stock solution of hIAPP was prepared by dissolving the lyophilized peptide in distilled water. The concentration of hIAPP peptides in the solution was determined by measuring the absorbance of the solution at 280 nm (ε = 1740 $M^{-1}cm^{-1}$) and then diluted at desired concentration into 20 mM HEPES, pH 7.5.[15,16] To prepare preincubated peptide samples, hIAPP (200 μM) was incubated in presence and absence of metal ions ($CuCl_2$ and $ZnCl_2$, 1.4 mM) at 37 °C with 300 rpm agitation. 1, 2, 3, and 9 h incubated samples were collected and stored at −80 °C.

4.4.2. Cell Viability Measurements. The rat insulinoma-1 (INS-1) pancreatic β cells were purchased from Addexbio. INS-1 cell line was maintained in media containing RPMI 1640 (GIBCO), 10% (v/v) fetal bovine serum (FBS, Sigma), 10 mM HEPES((4-(2-hydroxyethyl)-1-piperazineethanesulfonic acid), 1 mM sodium pyruvate(GIBCO), 50 μM β-metcaptoethanol (GIBCO), 100 U/mL penicillin and 100 U/mL streptomycin (GIBCO), 2 mM glutamine. The cells were grown and maintained at 37 °C in

a humidified atmosphere with 5% CO_2. Cell viability upon treatment of compounds was determined using the MTT assay (Sigma). Cells were seeded in a 96 well plate (30,000 cells in 100 μL per well). The cells were treated with or without hIAPP and $CuCl_2$ or $ZnCl_2$ in the absence and presence of compounds (calpeptin, trehalose, and bafilomycin; 1% v/v final DMSO concentration) and incubated for 24 h in the cells. After incubation, 25 μL MTT (5 mg/mL in phosphate buffered saline (PBS), pH 7.4, GIBCO, Grand Island, NY, USA) was added to each well and the plate was incubated for 4 h at 37 °C. Formazan produced by the cells was solubilized using an acidic solution of *N*,*N*-dimethylformamide (50%, v/v aq) and sodium dodecyl sulfate (SDS, 20%, w/v) overnight at room temperature in the dark. The absorbance was measured at 600 nm using a microplate reader. Cell viability was calculated in comparison to that of the untreated cells in percentage value (%).

4.5. References

(1) DeFronzo, R. A. *Med. Clin. North Am.* **2004**, *88*, 787–835.

(2) Hoppener, J. W., Ahren, B. & Lips, C. J. *N. Engl. J. Med.* **2000**, *343*, 411–419.

(3) Larson, J. L. & Miranker, A. D. *J. Mol. Biol.* **2004**, *335*, 221–231.

(4) DeToma, A. S.; Salamekh, S.; Ramamoorthy, A.; Lim, M. H. *Chem. Soc. Rev.* **2012**, *41*, 608–621.

(5) Marzban, L.; Park, K.; Verchere, C. B. *Exp. Gerontol.* **2003**, *38*, 347–351.

(6) Tanaka, A. *et al. Endocr. J.* **2009**, *56*, 699–706.

(7) Ma, L., Li, X., Wang, Y., Zheng, W., Chen, T. *J. Inorg. Biochem*. **2014**, *140*, 143–152.

(8) Ma, Z. A., Zhao, Z. & Turk, J. *Exp. Diabetes Res.* **2012**, 703538–703548.

(9) Rhee, J. S., Yu, I. T., Kim, B. M., Jeong, C. B., Lee, K. W., Kim, M. J., Lee, S. J., Park, G. S., Lee, J. S. *Aquatic Toxicol*. **2013**, *132*, 182–189.

(10) Jaikaran, E. T. & Clark, A. *Biochim. Biophys. Acta* **2001**, *1537*, 179–203.

(11) Casas, S.; Novials, A.; Reimann, F.; Gomis, R.; Gribble, F. M. *Diabetologia* **2008**, *51*, 2252–2262.

(12) Huang, C. J.; Gurlo, T.; Haataja, L.; Costes, S.; Daval, M.; Ryazantsev, S.; Wu, X.; Butler, A. E.; Butler, P. C. *J.Biol. Chem.* **2010**, *285*, 339–348.

(13) Rivera, J. F.; Gurlo, T.; Daval, M.; Huang, C. J.; Matveyenko, A. V.; Butler, P. C.; Costes, S. *Cell Death Differ.* **2011**, *18*, 415–426.

(14) Kim, J.Y.; Cheon, H. J.; Jeong, Y. T.; Quan, W.; Kim, K. H.; Cho, J. M.; Lim, Y. M.; Oh, S. H.; Jin, S. M.; Kim, J. H.; Lee, M. G.; Kim, S.; Komatsu, M.; Kang, S. W.; Lee, M S. *J. Clin. Invest.* **2014**, *124*, 3311–3324.

(15) Gill, S. C.; Hippel, P. H. *Anal. Biochem*. **1989**, *182*, 319–326.

(16) Pace, C. N. *Protein Sci*. **1995**, *4*, 2411–2423.

Acknowledgments

Completion of his thesis was impossible without the support of many people. I would like to express my sincere gratitude to all of them.

First of all, I would like to gratefully appreciate my advisor, Professor Mi Hee Lim, for giving me a great opportunity to do my master program in UNIST. She always supported me to keep doing my research work and gave consistent encouragement, valuable comments, and guidance despite her busy schedule. Without her commitment, I would not have completed my master program and this thesis would not have had the present performance and quality.

I am also grateful to the members of my committee, Professor Cheol-Min Park and Professor Kyung Taek Kim for sparing precious time, thoughtful insight, and valuable advice based on their expertise.

I thank especially Mi Sook Lim in that she has comforted and encouraged me during the course of my master program. I wish to special thank to Dr. Akiko Kochi. She spent time setting up our lab, teaching me many experiments especially cell culture, and took care of me. She is in Japan but I just want to say thanks and I wish her every success and happiness in her life. I also would never forget our lab members: Dr. Yeonju Kwak, Michael Beck, Hyuck Jin Lee, Kyle Korshavn, Younwoo Nam, Juhye Kang, Jeffrey Derrick, Jeeyeon Lee, Eunju Nam, Yonghwan Jee, and Jiyeon Han. I wish you all the best for your work and would be always happy. Thank you all!

Last, but foremost, I would like to appreciate my parents and my sister for their endless love, understanding, and support. Especially I am so proud of my mother enduring hard time this year. I love my father, mother, and sister so much!